UK Astronomy Technology Centre	ESO OWL

Document Title: OWL Instrument Concept Study - SCOWL

Document Number: OWL-CSR-ESO-00000-0163

Issue: 1.0

Date: 15 September 2005

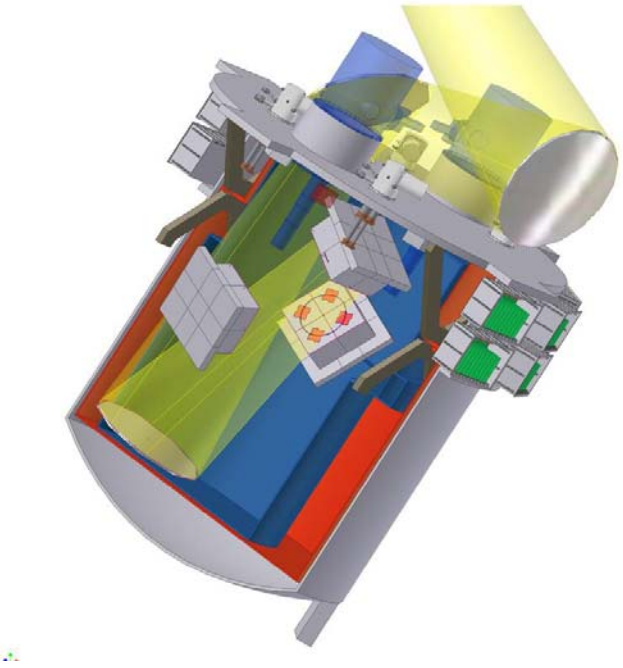

Document Prepared By

E Atad **D Gostick**
B Dent **W Holland**
I Egan **D Kelly**
M Ellis **R Siebenmorgen**

Document Released By: **B Dent SCOWL PI** **Signature and Date:**

Change Record

Issue	**Date**	**Section(s) Affected**	Description of Change/Change Request Reference/Remarks

Table of Contents

Figures

Tables

1 Introduction

This document describes an initial concept for a large-format sub-millimetre camera to be used on the OWL Telescope. Such an imager – dubbed SCOWL – would be unique, and the results would impact a wide range of research areas. It would help answer some of the most fundamental questions about the origin of dust, planets, stars and galaxies. As a result, the scientific return from the OWL telescope would be significantly increased. It would be able to detect dust in normal Milky Way Galaxies throughout the Universe, and detect planetary systems with dust masses lower than our own Solar System out to more than 20pc.

Some of the key questions which SCOWL would help answer are:

- How was dust formed in the early Universe?
- Why is our Solar System so free of dust: do we live in an unusual planetary system?
- Where is the bulk of dust in Galaxies? Is there an additional "cold, dark" massive component?
- How do high-mass stars form and how is their formation linked to the formation of Galaxies?
- What is the origin of the Kuiper Belt?
- What is the star formation history of different types of Galaxies, out to the highest redshifts?
- What is the origin of the low-level sub-mm background?

The subsequent engineering approach to fulfil the science case has been to provide a basic concept taking advantage of the technology and methodology being developed for SCUBA 2 - now considered the cutting edge of sub-mm instrumentation. Where there is a possibility that emerging technology might offer significant advantages, this too has been identified (e.g. KIDs development). Areas where a dedicated R&D approach would be needed are also identified (e.g. development of filter manufacturing capability).

2 Acronyms and Abbreviations

AIV	Assembly, Integration & Verification
CA	Clear Aperture
DRF	Dilution Refrigerator
FNO	Field Number
FoV	Field of View
FPU	Focal Plane Unit
GM	Gifford-McMahon
KIDs	Kinetic Inductance Detectors
LN2	Liquid Nitrogen
NEFD	Noise Equivalent Flux Density
NEP	Noise Equivalent Power
NIST	National Institute of Standards and Technology
PCB	Printed Circuit Board
PTC	Pulse Tube Cooler
PWV	Precipitable Water Vapour
SCOWL	Sub-mm Camera for OWL
SED	Spectral Energy Distribution
SMC	Scottish Microelectronics Centre
SQUID	Superconducting Quantum Interference Device
TES	Transition Edge Sensor
UK ATC	United Kingdom Astronomy Technology Centre

3 Applicable and Referenced Documents

	Title	Number & Issue
AD01	OWL Instrumentation Sub-millimeter Camera for OWL Technical Specification and Statement of Work	OWL-SPE-ESO-00000-0155 Issue 1.0 dated 22 Dec 2005
AD02	OWL Telescope-Instruments Interface Control Document	OWL-ICD-ESO-00000-0139 Issue 1.1 dated 25 Jan 2005
RD01	SCOWL: a large format sub millimetre camera on the Overwhelmingly Large Telescope Holland et al	SPIE 4840, 340
RD02	A large single-aperture telescope for sub millimetre astronomy Holland et al	SPIE 5489, 61
RD03	Adaptor-rotator draft concept	N.B. by S. D'Odorico -6 Jun 2005
RD04	Total power atmospheric phase correction at the SMA. Memo 154	Battat, Dec 2004
RD05	Note on "OWL Adaptive Optics Requirements for TOWL/SCOWL"	Email, V1.0, May 19, 2005
RD06	SCUBA-2 Array Technology Proof-of-Concept	Nov. 2002
RD07	Theoretical Modelling of Optical and X-ray Photon counting Kinetic Inductance Detectors. George Vardulakis, Stafford Withington, David Goldie	May 2005 SPIE 5499..348 2004
RD08	Frequency domain multiplexing readout of Kinetic Inductance detectors: Naidu Bezawada (UKATC)	May 2005
RD09	Multiplexable Kinetic Inductance Detectors: .B.A. Mazin, P.K. Day, J.Zmuidzinas, and H.G. Leduc	AIP Conf. proc.605, pp.309-312, AIP, New York, 2002
RD10	Superconducting Kinetic Inductance Photon Detectors: B.A. Mazin, Peter K. Day, Henry G. LeDuc, Anastasios Vayonakis and Jonas Zmuidzinas	SPIE 4849..283 2002

4 Science Case

The following outlines some of the exciting and competitive science that could be done with SCOWL. OWL is unlikely to be built until the middle of the next decade, so these cases are mainly based on projects in areas of current interest, along with some possible projected future science. It is not meant to be a "*roadmap*" of submm science in the next decade, but is structured to give an idea of the burning questions in astronomy that could be uniquely answered by SCOWL. For each topic, we provide an example project, and a list of specifications and requirements.

4.1 Baseline system assumptions

Some basic initial assumptions have been made about the telescope design, operation and site quality, as follows.

	Baseline value	Notes
Aperture (D)	100m	
Aperture efficiency (η_a)	0.6	Surface is effectively perfect at this wavelength, so η_a is limited by surface losses, geometrical blocking, and segment gaps.
"Workhorse" wavelengths	850μm 450μm 350μm	Another possible wavelength might be 200μm
Beam size (fwhm)	~1 arcsec	At 350 and 450μm
"Typical" precipitable water vapour content	1mm	PWV is lower than this for at least 25-50% of time
Field of view	2.5x2.5 arcmin	Larger FoV would allow faster mapping
Pixel spacing	Nyquist sampling (0.6λ/D) at 450μm	May be oversampled at 850μm
Pixel coverage	0.35 at all wavelengths	Fraction of science FoV that is covered by Nyquist-sampled pixels
Pointing/tracking accuracy	Better than 0.1"	1/10 of the smallest beam size
Strehl ratio	>80% Strehl ratio over full FoV	Optical Strehl
Observing time available for SCOWL	>30 nights	Number of nights per year when conditions are suitable for operation at "workhorse" wavelengths, and when telescope is not used for other work.

Table 1 Baseline system assumptions

4.2 Reference Science Cases

4.2.1 Solar system

As well as the Planets and Moons, the Solar System contains a significant mass of smaller objects such as Asteroids and Comets. *Understanding these objects is key to understanding the origin of the Solar System.* They can be subdivided into several different populations, such as Centaurs, TNOs, Plutinos, Scattered Disc Objects, KBOs; some are considered primordial from the formation of the Solar System, and others secondary, formed as the result of collisions. We need to explain the differences and origins of these populations, and how the objects are related.
To answer these questions we need to know:

- What are the size distribution and albedo of the populations? What are their total masses? With only optical/ir observations, the size can only be guessed at by assuming a fixed Albedo (e.g. Bernstein et al., 2004).
- What are the surface/regolith properties, such as thermal inertia, roughness and emissivity?
- What is the link to the short period comets?

Answers to these questions will come from study over a wide wavelength regime. Sensitive submm data are critical to understand and model the SEDs.

4.2.1.1 The Outer Solar System: Kuiper Belt Objects

The Kuiper Belt lies at ~30 to possibly >100au from the Sun, resulting in equilibrium temperatures of ~20-40K. *The submm is therefore the key wavelength regime for study of Kuiper Belt Objects.* The critical measurement of the size and Albedo of KBOs is possible by measuring fluxes at both optical and submm or far-IR wavelengths (e.g. Jewitt et al 2001). Currently this can be done on the very rare giant KBOs such as Sedna or Varuna, of diameters ~1000km or

larger. But their rarity means we may not be looking at where most of the mass of KBO material lies. Using the SCOWL sensitivity coupled with improved optical instruments, we can use this technique to study objects and derive the size distribution down to as small as 50km at distances of 50au. This size regime is very interesting for several reasons: as well as containing most of the KBO mass, it is below the cutoff diameter where bodies are no longer held together by gravitational force (e.g. Pan & Sari, 2005). They are approaching the sizes of classical comets, and may be the link between the two.

It is increasingly apparent that very distant bodies of masses at least that of Pluto do exist at the outer edge of the Kuiper Belt (eg Rabinowicz, et al., astro-ph/0509401). With SCOWL there is also an opportunity for serendipitous discovery of distant giant KBOs in the submm; this might be done during large-scale deep cosmological surveys taken over prolonged periods.

4.2.1.2 Asteroids

The submm fluxes of objects in the Asteroid Belt will allow us to measure sizes down to ~10m using a similar technique as described above. Furthermore the submm fluxes and SED can be used to estimate the surface properties of the regoliths, and the improved sensitivity will enable this to be done over a wide range of size scales.

4.2.1.3 Dust bands

Discovered by IRAS, these are the remains of collisions or breakup of comets and asteroids, and therefore may be local examples of "debris discs". Large-scale mapping of their structure and study of the more distant fainter, cooler bands would be possible. This will help understand the dynamics of these around external planetary systems.

Specifications

Parameter	Requirement	Desirable	Notes
Wavelength	350μm 450μm	850μm	Black-body emission
Sensitivity [1]	<0.1mJy (10σ)	<0.05mJy (10σ)	
Resolution	<2" at workhorse bands	1"	To avoid confusion limit
Field of view	20x20 arcsec		Not critical, as unresolved

4.2.2 Debris discs

At least 15% of main sequence stars are surrounded by dust that, at first sight, should not be there. This is because the dust removal timescale (through collisional erosion, or radiation pressure) are much shorter than the stellar ages, implying the dust must have been recently formed – possibly within the last few million years. The source of grains is thought to be mutual collisions and grinding down of larger bodies such as asteroids & comets. As well as being important for understanding the hidden population of such bodies in these systems, the distribution of this remnant dust is often sculpted by the orbital interaction with unseen planets; from their structures we can derive planetary masses and orbits, as well as their migration history (e.g. Wyatt, 2004). So the study of debris discs tells us not only about the dust content of exoplanetary systems, but also about bodies from planetary down to asteroids masses.

Existing studies of debris discs have been severely limited by three effects: instrument sensitivity, confusion against the nearby stellar photosphere, and background confusion. Consequently it has only been possible to investigate debris discs with unusually high dust content, such as Fomalhaut and ε Eri (see Figure 1b). The high sensitivity and spatial resolution of SCOWL will revolutionise this; Figure 2 shows that SCOWL will be able to detect dust masses

[1] "Sensitivity" in this and subsequent specification tables refers (except where noted) to the per pixel sensitivity at the "workhorse" wavelength after a "reasonable" amount of observing time, pointing at the same point on the sky (ie neglecting mapping requirements).

less than $10^{-5}M_{Earth}$ at a distance of up to ~20pc, and a disc similar to ε Eri to many hundreds of pc. This lower mass limit is particularly interesting, as it is approximately the mass of dust in our Solar System's Kuiper Belt – a system relatively free of dust and without a recent major collision. The number of targets within these distances is large (e.g. ~100 G stars; see http://nstars.arc.nasa.gov), and thus SCOWL will allow for the first time a snapshot of planetary systems in *all* stages after collisions and dust formation. An intriguing question to answer will be whether *most* stars have some debris, indicative of planets and asteroids? With SCOWL we will be able to answer this. An additional important contribution from such a survey is that missions such as Darwin/TPF will be significantly more sensitive to Terrestrial planets in the systems with low dust masses ($<10^{-6}M_{Earth}$; Beichman et al.., 2004). SCOWL will be an important pathfinder instrument for target selection.

SCOWL will be able to discriminate against stellar photospheric confusion, as the beamwidth (1") will resolve typical debris discs out to ~100pc. This ability to discriminate against the nearby stellar photosphere is one of the major advantages of SCOWL over far-IR surveys (those done with existing and all proposed 4-10m-class satellites; e.g. Decin, et al., 2003). Furthermore it has recently been shown by Spitzer that far and mid-infrared images of debris discs often bear little resemblance to the sub-mm images (Su et al., 2005); this is because the dust emitting at shorter wavelengths is significantly smaller and is being blown out by radiation pressure. In the sub-mm the 0.1-1mm (or larger) grains dominate; these are not affected by radiation pressure and so show the complex morphology seen in Figure 1. To observe the large (mm to m) grains trapped in resonances with planets or in rings, we must observe in the mm or sub-mm (e.g. Wyatt et al., 2005, Su et al., 2005). SCOWL will therefore provide a unique combination of high sensitivity and adequate resolution to study these grains in all nearby stars. *By combining debris disc studies with the direct optical/infrared observations of planets planned with OWL, we will obtain a complete inventory of the rocky and gaseous bodies in distant planetary systems.*

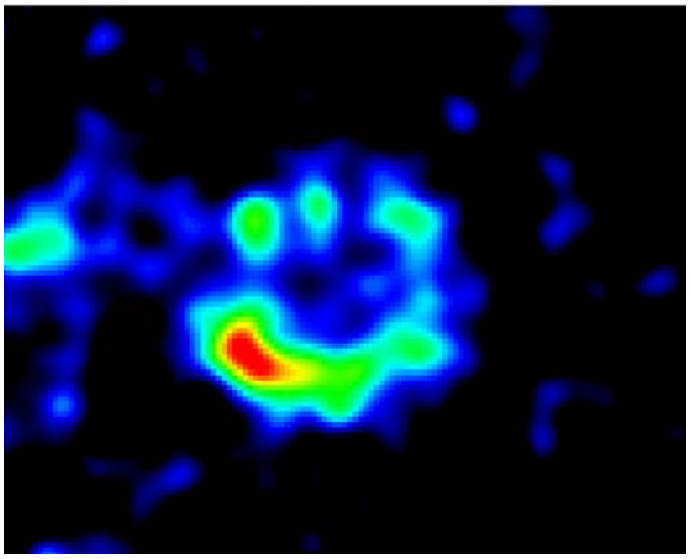

Figure 1a

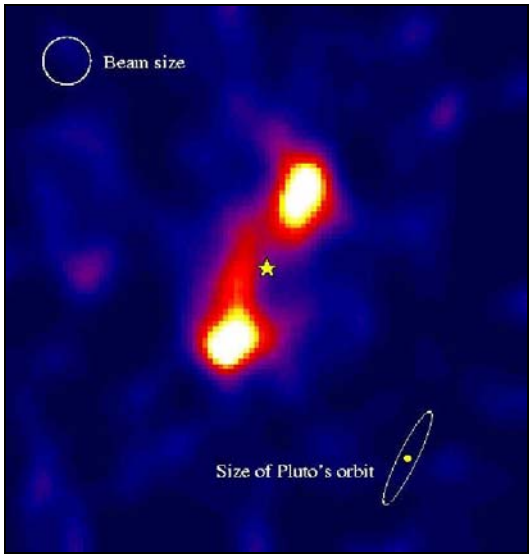

Figure 1b

Figure 1: SCUBA/JCMT images of Fomalhaut and ε Eridanus, two of the closest and brightest debris discs - at 850um. Resolution is 14 arcsec, or 45au at the distance of ε Eri (3.2pc). SCOWL will resolve such discs to distances of 100pc, with masses 100-1000x lower – around that of the Solar System.

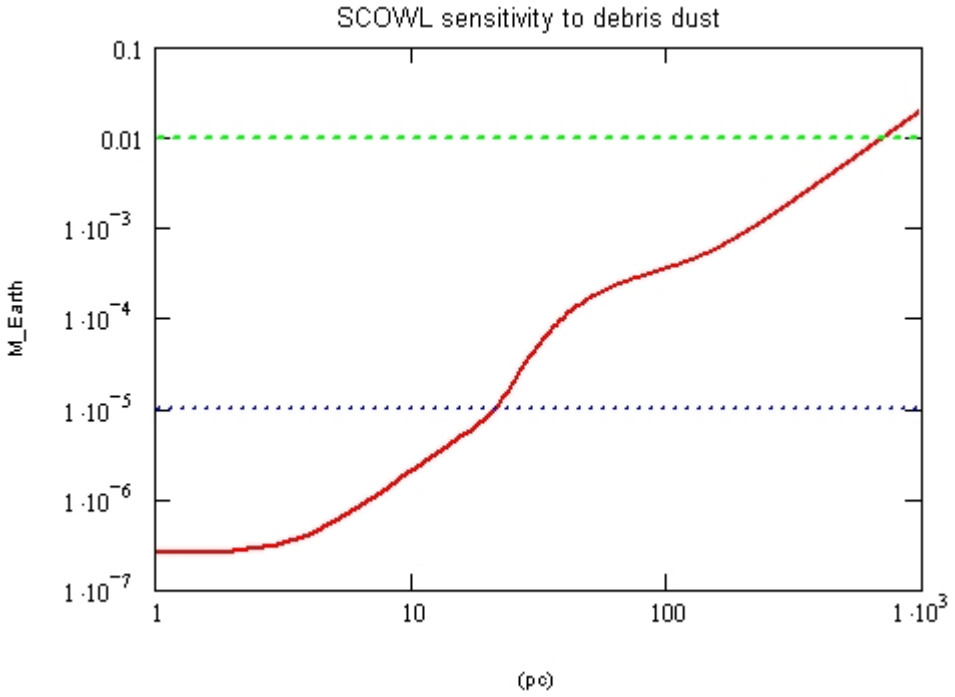

Figure 2: Red line represents the detection limit of SCOWL (10σ) as a function of distance, for a $3L_{sol}$ star, with 3 hours of integration time. Dust masses are in units of Earth masses. The upper and lower lines are the dust masses of E Eri and the Solar System respectively.

Some of the key questions to answer are:

- Do *all* stars have debris (and by inference, asteroids)?
- Is the Solar System an unusually dust-free case, or is there a continuous distribution of dust masses?
- What is the typical long-term evolution of debris around stars? Spitzer suggests that little changes after the first ~200Myrs of a stars' life, apart from random collisions; however, this is sensitivity-limited. A deep survey is required over a wide age range.
- Does the stellar location and evolution affect the debris disc? Are stars formed in dense environments more likely to have debris?
- Does the stellar mass, metallicity and multiplicity affect debris mass?
- How is the dust alignment affected by the stellar magnetic field (through submm polarimetry – see section 4.2.6)

Specifications

Parameter	Requirement	Desirable	Notes
Wavelength	850μm 450μm (simultaneously)	350, 450, 850μm (simultaneously)	
Sensitivity	<0.1mJy (10σ)	0.05mJy (10σ)	
Resolution	<2" at workhorse band	1"	For discrimination against photosphere
Field of view	2x2 arcmin	4x4 arcmin	Nearest discs are ~60-100" diameter
PSF accuracy	Can be calibrated (i.e. is stable) to better than 1% over region from 1-10 arcsec	Better than 0.5% over 1-60 arcsec	To allow measurement of faint emission near star, the sidelobes must be low level, and stable.
Observing mode	Mapping FoV	hitchhiker mode preferred	

4.2.3 Planet formation

4.2.3.1 Transitional discs – the last stages of planet formation

The last vestiges of primordial circumstellar discs, around stars of 1Myr to a few 100Myr, are of great interest, as it is in these that planets will be forming. In our own Solar System, this came to an end with the "Age of Heavy Bombardment", where the planets had formed and were impacted by large bodies from the remnant disc. As well as understanding this formation mechanism itself, we also need to explain the evolution from this to the population of evolved exoplanets: how does this dust disappear?

Key questions in this area are:

- What are the timescales of dust removal around young stars? Does the primordial dust exist for prolonged times around stars? How is this dust related to the "age of heavy bombardment" in the Solar System, and is such a phenomenon common to most young planetary systems?
- What is a "typical" planetary system, and how does it get to its current state?
- What is the fundamental origin of the distribution of planetary masses and distance? How is this related to conditions and evolution in the early disc?
- Why do many exoplanets have high eccentricity? Is the Solar System rare in its low planetary eccentricities? This may be related to the prevalence of dust/gas during the early phase of a planet's life.

4.2.3.2 Disc evolution

It is becoming recognised that the evolution of young stars can be widely different: Weak-line T Tauri stars can have little dust compared to their Classical counterparts, yet be of the same age. Why do some stars lose their disc within the first 10^5 yrs, yet others have ones that last for 10Myr or more? Also there is clear evidence that large grains (≥1mm) do exist in many older discs (e.g. Testi et al., 2003): one of the clearest ways to measure this is by looking at the sub-mm spectral slope. However, it is unclear whether this indicates gradual grain growth, or different balances between coagulation and fragmentation (Dullemond & Dominik, 2005). What might affect such balance differently in different objects is unknown, but both effects are likely to have profound impacts on the formation of any larger bodies within these systems.

To answer these questions, deep, whole-cluster surveys are required to track the statistics of all cluster members, with total masses down to the substellar limit. Clusters have sizes of a few arcmin up to ~1 degree for the closest (150pc, Figure 4).

Specifications

Parameter	Requirement	Desirable	Notes
Wavelength	350μm, 450μm, 850μm		Multiple wavelengths to get SED
Sensitivity	0.1mJy (10σ)		
Resolution	<2" at workhorse band	1"	Confusion limit in crowded clusters
Field of view	2x2 arcmin	10x10 arcmin	Wide-field mapping of 1-300Myr clusters

4.2.4 Star formation

4.2.4.1 Formation of the lowest mass stars

What is the mass function of protostellar clumps down to the sub-stellar limit? Does this affect the IMF of stars, potentially explaining the so-called "free-floating" planets? This requires large-scale, deep and high-resolution surveys of the closest star formation regions. Currently the deepest large-scale maps reach 10σ limits of ~0.1Jy at 850μm (e.g. Johnstone et al., 2000). With SCOWL, we can reach 10σ limits of 1mJy - *at 450μm* (where the dust flux is higher) – and covering 1 degree square in a few hours (and a factor of 2-3 lower at 850μm). At this level, the main limitation will be confusion from the background galaxies; techniques such as differential number counts compared with nearby clear sky, and source identification through submm colours (which by that time should be accurately known through templating), will be used to help reduce this confusion limit. The pure sensitivity limit corresponds to a 10σ detection of a $0.1M_{Jupiter}$ clump in Orion. So with SCOWL we will be able to extend the clump mass spectrum in Figure 3 down by a factor of ~100, and possibly 1000. *SCOWL will provide a complete clump census down to planetary masses in regions out to 2kpc.*

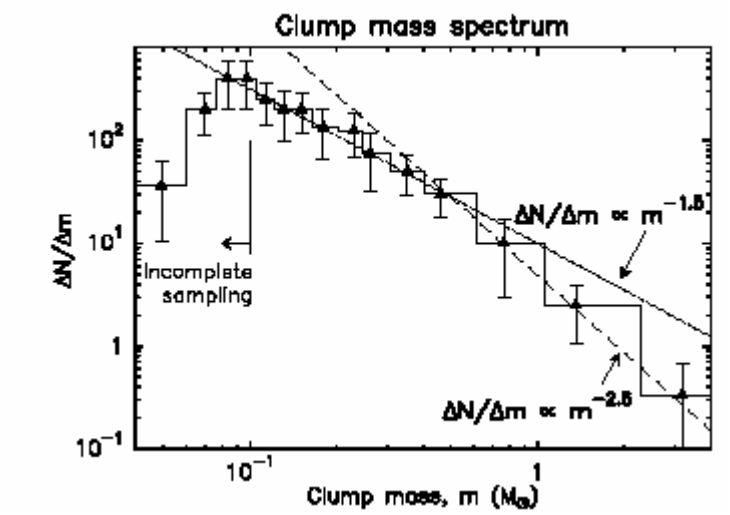

Figure 3 The clump mass spectrum of cores in Ophiuchus (from Andre et al., 1998). Note that this is incomplete below $0.1M_o$.

4.2.4.2 Solar-mass star formation

It is clear that the ability to map star forming regions in the submm dust continuum has provided extremely valuable insights into *local* star formation (i.e. in low-mass formation in clusters within 150pc, and high-mass formation within ~500pc). This is illustrated by the map of ρ Ophiuchus (Figure 4). But we need to extend these local studies to understand star formation in the Galactic context. The combination of sensitivity, reasonable resolution and wide-field mapping with SCOWL will allow for the first time, surveys of clusters as far as the Galactic Centre. The deepest studies of Brown Dwarfs in the nearby Trapezium cluster indicate a mean stellar separation of ~0.04pc (Lucas et al., 2005); this would correspond to 1 arcsec at the Galactic Centre. Cluster sizes of a few arcmin could be mapped to 1mJy (10σ), corresponding to $10M_{Jupiter}$ at this distance.

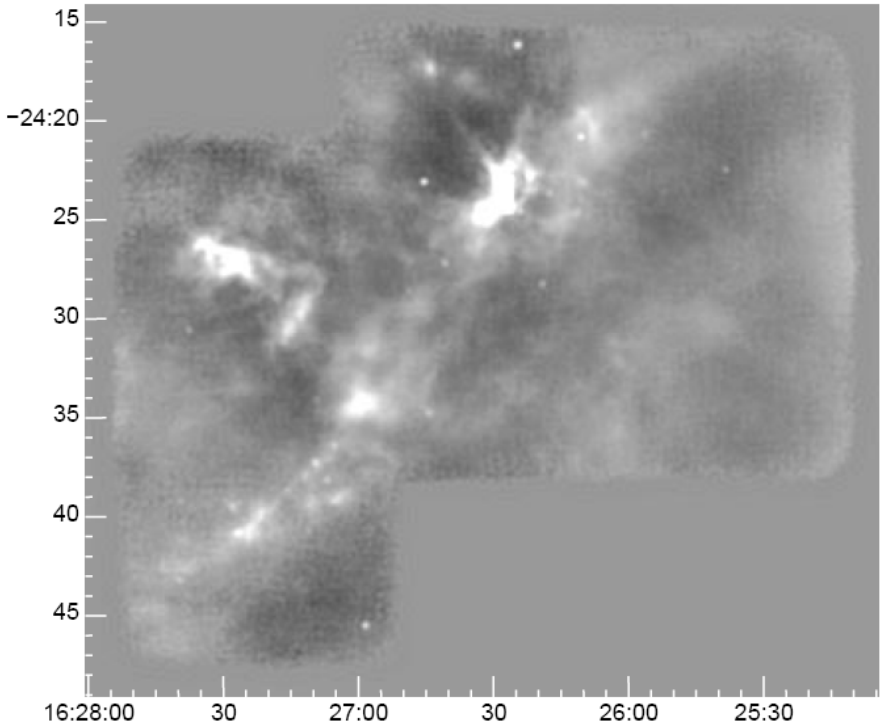

Figure 4: SCUBA map of nearby star forming region (rho Ophiuchus, from Johnstone et al., 2000). 55 cores down to masses of 0.02Msol are identified in this image. SCOWL will be able to study clusters similar to this throughout most of the Galaxy.

Some of the key areas to study:

- What is the difference between high and low-mass star formation processes?
- How does the star formation process differ in high metallicity areas, and regions of high Galactic shear and turbulence (e.g. towards the Galactic Centre)?
- What are the important parameters affecting star formation in clusters? Is cluster density important in YSO evolution?
- What is the fundamental cause for initial collapse: is it turbulence, or direct response to some large-scale phenomenon?

4.2.4.3 Proto-binary systems

Most stars form in some kind of binary or higher-multiple system, but the evolution of proto-multiples is very poorly known. At early times, the protostars share a common circumstellar envelope or even a circumbinary accretion disk, but arcsecond resolution is needed to image such systems. Nearby star formation regions such as those in Ophiuchus

and Taurus (150pc distance), so wide proto-binaries (~1000 AU) would easily be resolved with an arcsecond OWL beam (corresponding to 150 AU). Furthermore, the sensitivity would be greater than that available with interferometers (e.g. ALMA), with the advantage that large-scale emission would be detected directly. This will give a unique picture of the earliest stages of a proto-multiple star system as it emerges from the parent cloud, and vital clues to how the multiplicity is determined (e.g. by core fragmentation). These studies would quantify the protostar numbers and masses within a group down to very low (sub-stellar) limits, and also show whether the inter-star spacings evolve with time. For example, dynamical interactions may eject group members even at the earliest protostellar stages.

4.2.4.4 Controlling the Interstellar Medium: High-mass star formation

Massive stars are rare, but their effect on the ISM is dramatic. Their winds and outflows are thought to define the lifetime of Giant Molecular Clouds, limiting the possibilities of subsequent star formation, and controlling disc and planet formation around stars in clusters such as Orion. *Any global model of star formation, and any model of Galaxy formation requires an understanding of high-mass star formation.* However, the early stages of high-mass star formation are not understood, partly because they are so fast and consequently rare. A full census of all high-mass star formation throughout the Galaxy will be feasible with SCOWL, as the 1" resolution will resolve OB clusters to 20kpc. The resultant statistics will show the rarest of phases, and allow us to understand what defines the highest-mass end of the stellar IMF.

Specifications

Parameter	Requirement	Desirable	Notes
Wavelength	350μm 450μm	850μm	To get more accurate mass, need 850μm flux as well, to be less dependent on temperature.
Sensitivity	1mJy (10σ) over a large-field (degrees).	0.1mJy (10σ) over a small field (5 arcmin)	Number counts limited by background confusion
Resolution	<2" at workhorse band	1"	To avoid local confusion limit in crowded distant clusters
Field of view	2x2 arcmin	4x4 arcmin	Wide-field mapping of OB star-forming regions.

4.2.5 The origin of dust: supernovae and evolved stars.

Submillimetre astronomy relies on the existence of interstellar dust, but surprisingly very little is known about its origin. It is generally assumed that about half the dust in the interstellar medium has been produced in supernovae, but there is almost no evidence that this is the case. In the early universe, the problem with the alternative dust formation mechanism – winds from evolved stars – is that these take too long (e.g. Edmunds 2005). There is clear evidence that the Universe was already very dusty even at redshifts of 5 or greater (see section 4.2.12).

The ideal way to test this is to observe dust in supernovae remnants which are young enough that little dust will have been swept up from the ISM, but even young supernova remnants are too large and with too low surface brightness to be mapped with current facilities. Only two (Cass A – see Figure 5, and Kepler) are bright enough to even consider mapping at 850μm; however, these data are controversial because of potential confusion with unassociated dust in the line of sight (Krause et al., 2004). Another problem is that the synchrotron emission is significant and dominates the 850μm images (see Figure 6). To help solve these problems would require large-scale mapping at λ~450μm (as well as 850μm) with high spatial resolution to identify the extended dust emission in the SNR.

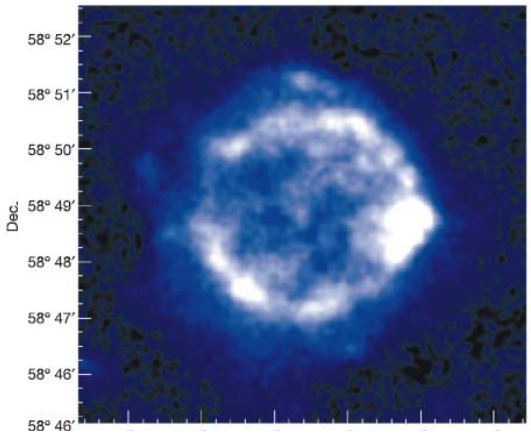

Figure 5: image of Cass A SNR at 850μm (Dunne et al., 2003).. Note that the image is dominated by synchrotron emission (see text for details).

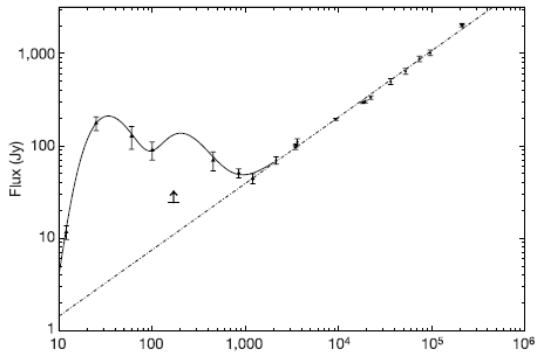

Figure 6: Spectral Energy Distribution from Cass A (Dunne et al., 2003). Only at wavelengths between 100 and 450μm does the emission from cool dust dominate over the synchrotron radiation.

The other potential source of dust - evolved stars - produce extended dust shells that are detected many arcminutes from the parent stars. However, since episodic violent ejection can produce rings of enhanced emission only a couple of arcseconds thick, *SCOWL would be unique in imaging not only the entire shell but also resolving the ring-like features*. High-resolution imaging would trace the inter-ring spacings, and thus show if episodic ejection occurs on regular or random timescales, and (from the ring width and measurements of the expansion velocity) for how long these episodes last. Although dust is produced by such post-main sequence stars, the physics is poorly understood. Are the shells clumpy, for example, with dust formed only in the densest regions? What are the production rates? Does the dust survive as it meets the harsh interstellar environment at the outer boundary of the envelope? High-resolution imaging is the only way to measure the dust masses in small clumps and a wide field plus high sensitivity is necessary to measure the faint tail of dust at the outer edges of these nebulae. SCOWL will be ideal for mapping both types of object - and thus answering the question of where and how dust is formed.

Specifications

Parameter	Requirement	Desirable	Notes
Wavelength	450μm, 850μm	350μm	Shorter wavelengths and spectral slope to discriminate against synchrotron emission.
Sensitivity	1mJy (10σ)	0.1mJy (10σ)	Extended emission
Resolution	2" at workhorse band	1"	More detailed structure and comparison with high-resolution synchrotron maps helps discriminate against other dust along line of sight.
Field of view	2x2 arcmin	4x4 arcmin	Wide-field mapping SNRs

4.2.6 Polarisation of dust

Aligned spheroidal dust particles produce at low frequencies very substantial polarised emission. Even when the grains have small elongation (axial ratio ~1.4) the polarisation reaches ~20% and higher values can be observed for more cylindrical dust. The wavelength dependence of the polarisation is flat in the far IR and submm and does not vanish for arbitrarily small optical depths. This is quite contrary to polarisation by dust extinction. If one detects towards a dust cloud polarised submm radiation and simultaneously polarised light at much shorter (optical) wavelength from embedded or background stars, one would notice that the polarisation vectors associated with these two processes, emission and extinction, are perpendicular to each other. The ratio of the submm and visible polarisation provides unique information to constrain the shape of the dust particles. The dust geometry and the elongation parameter of the grains in particular, is directly related to the submm extinction property. Knowledge of the submm extinction is most important as it is widely used to measure the conversion of flux to dust mass. But with current instruments the relatively low angular resolution and sensitivity, limit sub-mm polarimetry to only the very brightest regions of clouds. Today, star formation regions have been detected with polarisation from ~1% in unresolved central clumps, up to ~20% in the resolved outer regions (see Figure 7).

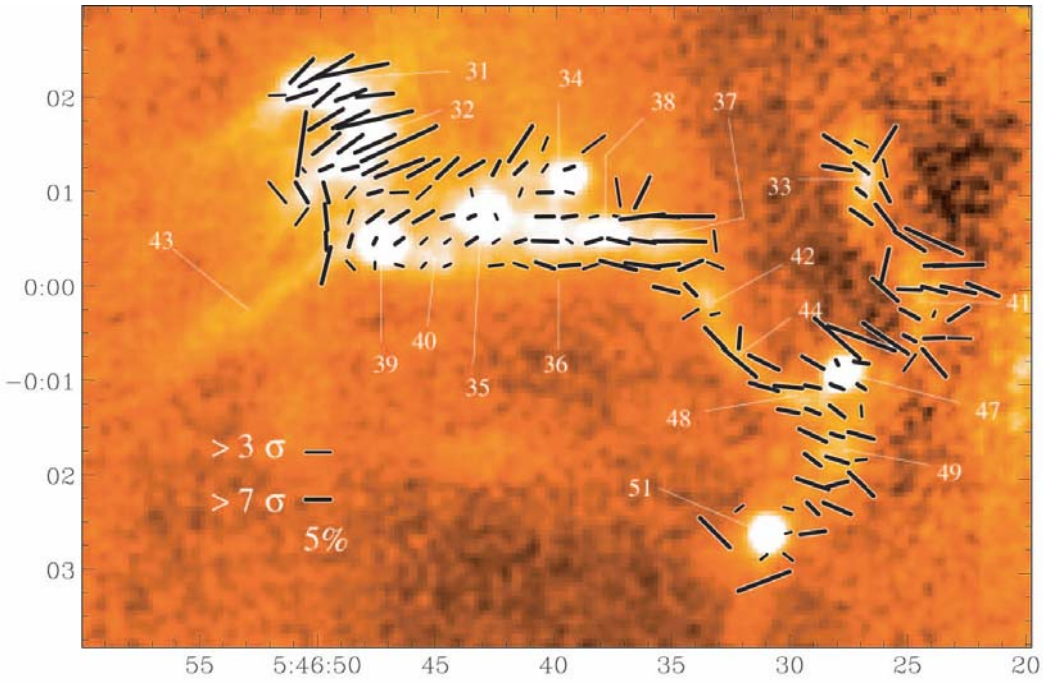

Figure 7: polarisation of 850μm continuum from the NGC2068 star formation region (Matthews & Wilson, 2000). Y-axis scale is in arcminutes. Complex structure can be seen, frequently unresolved by the beam (14 arcsec), at a high level of polarision (up to 12%).

The fractional polarisation and angle provides *unique* information about the dust alignment, magnetic field structure, and grain structure and elongation that is unavailable at other wavelengths. The extreme sensitivity, angular resolution and wide field of SCOWL will allow us to measure polarisations of regions which can currently only just be detected at sub-mm wavelengths. It also provides high spatial resolution to investigate the detailed magnetic field structure.

An example of the use of such an instrument would be to measure the polarisation of debris discs, to investigate dust grain alignment mechanisms within these systems. For the extended disc of ε Eri (see Figure 1), the fainter emission is ~8mJy/beam at 850μm, or ~0.2-1mJy/beam with SCOWL (assuming extended emission, with some degree of clumpiness). Discs out to distances of ~tens of pc would have similar surface brightness level. For 5% polarisation, this would imply ~10-50μJy polarised flux per beam at 850μm. This would be detected to ~3-20σ in 10 hours with SCOWL.

Specifications

Parameter	Requirement	Desirable	Notes
Wavelength	450, 850μm (simultaneously)	350, 450, 850μm (simultaneously)	850μm is more desirable than 350μm, as polarimetry requires a more stable atmosphere than photometry.
Sensitivity	<0.05mJy (10σ) polarised flux at 850μm (<1% pol. of a *total* flux of 5mJy at 850μm)	<0.05mJy (10σ) polarised flux at 450μm (<1% pol. of a *total* flux of 5mJy at 450μm)	Polarised flux would be higher at 450μm by a factor of ~3-6, from typical dust spectral index
Instrumental polarisation	<1% stable to <0.2%	<0.5% stable to <0.1%	subject to calibration plan
Resolution	<2" at workhorse band	1"	
Field of view	2x2 arcmin	4x4 arcmin	

4.2.7 Completing the census of the Galaxy: a submm galactic plane survey

There is *no* survey of the entire Galactic Plane in the submillimetre continuum (at even the crudest resolution). Currently the best available data are the 8-arcminute resolution maps of optically thick emission from CO molecules (Dame et al., 2000). Since dust is a much better unbiased mass tracer, a submillimetre Galactic Plane survey will give a true census of the star-forming cloud population and the total mass of cold dust in our Galaxy. At the moment, more is known about the dense clouds in Andromeda Galaxy than about those in the Milky Way. In the next few years, large-scale surveys with SCUBA-2 on JCMT will trace dust down to several tens of mJy. But with SCOWL a 180 x 2 degree Galactic Plane survey to a 1σ depth of 300 μJy would take only 10 nights, and would detect (and possibly resolve) not only the coldest pre-stellar core population but would detect cores down to only a few Jupiter masses at distance of the Galactic Centre. Such a survey with SCUBA-2 on the JCMT is well below the confusion limit of a 15-m telescope and would take many thousand years - even if it were possible!

Specifications

Parameter	Requirement	Desirable	Notes
Wavelength	450μm 850μm	350μm	
Sensitivity	3mJy (10σ)		Very large-scale mapping (360 sq. degree)
Resolution	<2" at workhorse band	1"	Sets confusion limit in galactic centre and along spiral arms.
Field of view	2x2 arcmin	4x4 arcmin	Wide-field mapping, so maximise the number of pixels.

4.2.8 Cold dark matter in Galaxies

The only reliable way to trace the bulk of dust in Galaxies is through submm imaging. It is becoming clear that most of the dust mass in spiral Galaxies lies in extremely cold, low-surface brightness disks, often extended far from the galactic nucleus. Submm spectral energy distributions show dust temperatures around 10-20K (Siebenmorgen et al., 1999; Stevens et al., 2005).

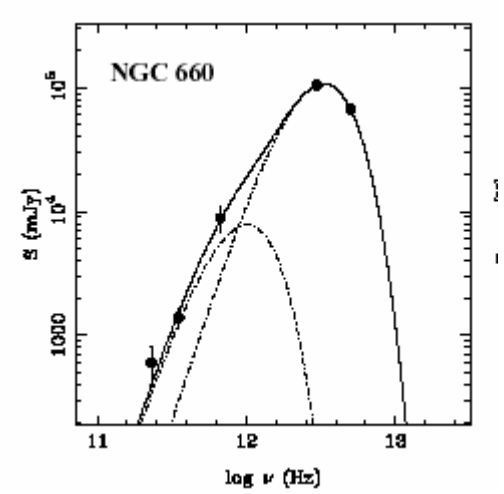

Figure 8 Spectral energy distribution of a typical spiral galaxy. Most of the submm emission is from a cold dust component at T~20K (Stevens et al., 2005).

Such cold dust radiates strongly in the submillimetre, but is orders of magnitude fainter in the far-infrared (Figure 8). Understanding this component is critically important, as it dominates the total dust mass. How far it extends beyond the stellar disc and the relationship to the Galactic ISM is unknown. How much this cold material contributes to the total mass at large radii, and hence how it affects the rotation curve is also unclear. In terms of studying this material in the Local Universe, 1 arcsec at z ~ 0.1 (distance of ~500Mpc) corresponds to a resolution of 2.4kpc and a survey of cold dust would resolve a population of galaxies to z ~ 0.1 – around the limit of the all-sky Schmidt surveys.

Furthermore, the imaging power and resolution achievable with SCOWL would allow the study of individual giant molecular clouds far from the galactic nucleus in nearby galaxies. This would address unique issues such as whether molecular cloud-cloud shielding or high HI optical depth can result in substantial underestimates of the gas surface density, and hence seriously compromising optical studies of star formation efficiency. In addition to studying individual nearby galaxies, SCOWL will be vital for determining the low-z benchmarks, such as the local luminosity and dust mass functions, which are needed to interpret information from the deep cosmological surveys. This requires mapping of substantial portions of the sky, but poor resolution and sensitivity have hampered surveys of this kind with IRAS and subsequent missions.

Understanding the mass distribution of interacting Galaxies is important, as this may be the way that Galaxies formed in the early Universe. SCOWL will be a vital tool to map cool dust in interactions in the local universe (out to distance of 500Mpc).

Specific questions to answer are:

- How is the cold dust distributed in nearby Galaxies? Does it extend beyond the warm dust or star forming disc?
- How much does the cold component contribute to the dark matter content?
- How do Galaxies interact? Is there a significant cold dust/gas component we are currently missing in interacting galaxies?

Specifications

Parameter	Requirement	Desirable	Notes
Wavelength	350μm 450μm	850μm	
Sensitivity	0.1mJy (10σ)	0.05mJy	
Resolution	<2" at workhorse band	1"	
Field of view	2x2 arcmin	4x4 arcmin	Mapping of nearby spirals and interactions

4.2.9 Intergalactic medium

Galaxy Clusters with massive central Ellipticals have a hot extended X-ray halo, often many arcmin across in the closer objects. This was originally thought to be a cooling flow, and is likely linked to dark-matter haloes. In many cases this emission is thought to have a significant and possibly extended *cold* component; gas has been observed using CO in some of the brightest objects (e.g. Edge, 2001). However the masses are extremely uncertain, and in most cases, the dust is somewhat underabundant and therefore too weak to detect - let alone map - with existing instrumentation. But it is not clear whether this cold material is linked to possible mergers, rather than the cooling flow.

How significant is the mass of this cold component? Is it primordial? What is its' distribution compared with the X-ray observations? These can be answered by deep extended mapping of in the sub-mm, looking for the cold dust component. The resolution must be sufficient to separate out the Galaxies themselves, leaving only extended dust. This is a project ideally suited to the high mapping sensitivity and FoV of SCOWL.

4.2.10 Galaxy formation

The negative K-correction for dust emission in the sub-mm passband (Blain & Longair 1993) means that an extremely luminous, dusty starburst with bolometric luminosity of 10^{13}Lsolar would have an 850μm flux of ~10 mJy (within a factor of ~2) if observed at *any* redshift between 1 and 10. Hence the sub-mm provides access to the Universe at epochs as early as only 5% of its present age. This is illustrated in Figure 9, which shows the SED of M82, a nearby luminous galaxy, at various redshifts.

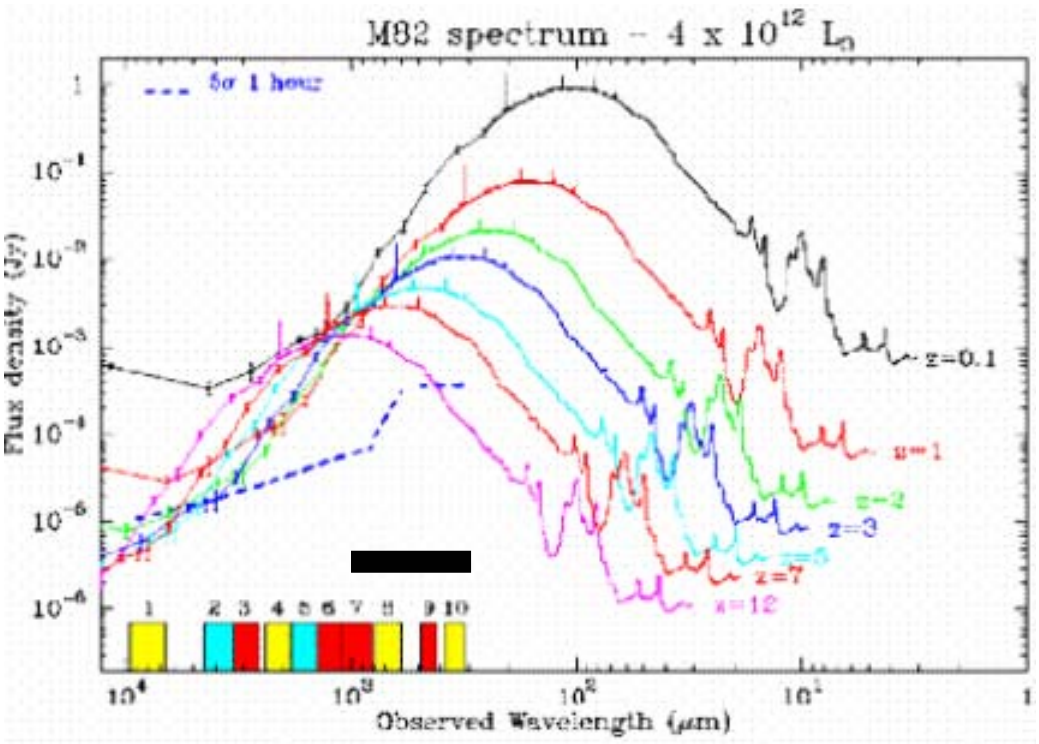

Figure 9: Spectral energy distribution of M82 observed at various redshifts. The wavelength range of SCOWL is indicated by the black bar

At wavelengths other than the sub-mm, the effects of cosmological dimming mean that it rapidly becomes extremely difficult to detect ever more distant galaxies, and it can prove virtually impossible to determine whether or not galaxies do actually exist at extreme redshift z > 5. Unbiased surveys of various sizes and depths – the "wedding cake" approach - are crucial for studying the formation and evolution of galaxies. Although SCUBA has radically changed our view of early star formation, current surveys have only uncovered a few hundred submm-selected galaxies. During the next decade instruments such as SCUBA-2 on JCMT will extend this to more statistically reliable samples. However, the confusion limit for 15m-class telescopes means that such surveys can only detect the most extreme objects - rare, massive galaxies forming over 1000 solar masses of stars every year in the early Universe (z>3). SCOWL would not only give a vast increase in mapping speed over any other planned facility, but would be able to probe and importantly find new objects down to much lower star formation rates than current single-dish telescopes. For example, a $1L_*$ galaxy at z=3 would have an 850μm flux of 10-100μJy, easily detectable with SCOWL. *SCOWL will therefore give us the ability to detect galaxies with star formation rates similar to the Milky Way throughout the Universe*. Unbiased samples of galaxies could therefore be assembled very rapidly. Moreover, to probe the evolution of more normal galaxies, such as the U, B and V-dropouts that are believed to be the precursors of modern-day disk galaxies, it is necessary to probe below the present confusion limit to few tens of μJy. This could be achieved with SCOWL in only a few hours.

In addition, the ability to simultaneously measure the 850, 450 and 350μm fluxes provides a reliable way of estimating the redshift to within ±0.4 or better (e.g. Hughes et al., 2002). This can be seen in the differences in sub-mm curvature of the template SEDs in Figure 9; it is not possible to do this at λ>1mm except for redshifts ≥20. Furthermore the severe confusion limit with the small apertures of far-IR satellites causes problems with cross-identification of objects at multiple wavelengths. Indeed in the absence of extremely deep infrared/optical or time-consuming sub-mm spectroscopic searches, sub-mm photometry at high angular resolution may be the *only* way to constrain z.

Specifications

Parameter	Requirement	Desirable	Notes
Wavelength	850μm, 450μm	350μm	Shorter wavelengths do not have K-correction advantage at z>5. But can be used to constrain redshift.
Sensitivity	0.05mJy (10σ)	0.01mJy (10σ) at 450μm	Sensitivity whilst mapping field-of-view. Desirable is to reach 1σ/1beam confusion limit.
Resolution	<2" at workhorse band	<1"	To provide lowest confusion limit
Field of view	2x2 arcmin	4x4 arcmin	

4.2.11 Large-scale clustering

The ensemble of existing extragalactic surveys with SCUBA have successfully resolved the bulk of the submillimetre background (e.g. Blain et al., 1999), established the importance of dust-obscured star formation in the early Universe, and investigated the clustering of the most active galaxies on scales up to 1Mpc. Attention has now shifted to the fundamental nature of submillimetre galaxies and their role in the history of structure formation: do bright submillimetre sources really represent forming ellipticals, or merely short-lived bursts of violent activity in the progenitors of more modest galaxies? What is their relationship, if any, with high-redshift optically selected galaxies? Wide-field surveys with sensitivities well below the current confusion limit are required to address these issues. If bright submillimetre galaxies are indeed the progenitors of massive ellipticals then they should be strongly clustered, with scale lengths of around 10Mpc (roughly 30 arcmin). A survey covering 10-100 square degrees with a rms sensitivity of a few hundred μJy is thus required, and this can *only* be done with SCOWL. Such a survey would detect many less luminous galaxies (currently selected only in the optical), allowing their clustering to be properly assessed, unbiased by obscuration, and compared with modern-day galaxy populations. Since massive ellipticals dominate the cores of rich galaxy clusters, such surveys will provide an important tracer of the growth of large-scale structure in the very early universe.

Specifications

Parameter	Requirement	Desirable	Notes
Wavelength	850μm, 450μm	350μm	Shorter wavelengths can be used to constrain redshift.
Sensitivity	1mJy (10σ)	0.1mJy (10σ)	Sensitivity for mapping 100 square degrees
Resolution	<2" at workhorse band	<1"	

4.2.12 Cosmic star-formation history.

It is known from studies of the Cosmic Microwave Background that the universe started off in a very uniform state, with no real structure. At some point the "Cosmic Dark Ages" came to an end through the birth of the first stars within primordial galaxies. Nuclear energy was converted to light in stellar interiors, and had important heating and ionisation effects on the surrounding medium. Exactly how this process began and subsequently evolved is one of the greatest cosmological puzzles. Recent work in the submillimetre has shown that luminous infrared galaxies evolve more strongly than their more normal optically-bright counterparts. It has also become clear that luminous obscured galaxies at high redshift contribute a substantial fraction (arguably the majority) of the total emitted radiation in the Universe. Roughly half of all the stars that have formed by the present day have probably formed in highly obscured systems. To trace the star-formation history of the various classical galaxy types (ellipticals, spirals) over cosmic history with sufficient precision would require a sample size of around 1 million galaxies. A large project such as this would require mapping 10 sq. degrees to 0.02mJy (1σ) sensitivity at 850μm; this could be achieved in a few weeks observing with OWL. The high spatial resolution would yield accurate galaxy positions, whilst simultaneous 850 and 450μm measurements (and preferably also 350μm of the brightest) would allow photometric redshifts to be obtained.

Specifications

Parameter	Requirement	Desirable	Notes
Wavelength	450μm, 850μm, 350μm		Multi-wavelength to get redshift
Sensitivity	0.2mJy (10σ) at 850μm	0.2mJy (10σ) at 450μm	Over 10sq.degrees
Resolution	2" at workhorse band	1"	
Field of view	2x2 arcmin	4x4 arcmin	Larger is better

4.3 References

Beichman et al., 2004, Advances in Space Research, vol.34, Issue 3, p. 637

Bernstein et al., 2004, ApJ 128, 1364

Blain et al., 1999 ApJ 512, L87

Blain & Longair, 1993, MNRAS 264, 509

Decin et al., 2003, ApJ, 598, 636

Dullemond & Dominik, 2005, A&A, 434, 971

Dunne et al., 2003, Nature, 4242, 285

Edge, 2001, MNRAS, 328, 762

Edmunds, 2005, George Darwin Lecture, A & G, 46, p412

Greve et al., 2004, MNRAS 354, 779

Helou & Beichman 1990, in ESA, From Ground-Based to Space-Borne Sub-mm Astronomy p 117-123

Hughes et al., 2002, MNRAS, 335, 871

Jewitt et al., 2001, Nature, 411, 446

Jeoung et al., 2005, MNRAS 357, 535

Krause et al., 2004, Nature, 432, 596

Lucas et al., 2005, MNRAS, 361, L211

Matthews & Wilson, 2000, ApJ 531, 868

Motte et al., 1998, A&A 336, 150

Pan & Sari 2005, Icarus, 173, 342

Pearson, 2001, MNRAS, 325, 1511

Siebenmorgen et al., 1999, A&A 351, 495

Su et al., 2005, ApJ, 628, 487

Stevens et al., 2005, astro-ph/0411721

Takeuchi & Ishii, 2004, ApJ, 604, 40

Testi et al., 2003, A&A 423, 323

Wyatt et al., 2005 (in prep)

4.4 Final summary specifications

Parameter	Requirement	Desirable	Notes
Wavelength	850μm 450μm 350μm (simultaneously)		
Sensitivity	<0.1mJy (10σ) (at 850 and 450μm)	Same sensitivity over whole FoV (ie fully populated FoV)	10σ, 1hr, point source
Resolution	<2" at workhorse bands	1"	
Field of view	2x2 arcmin	4x4 arcmin	
PSF accuracy	PSF can be calibrated (i.e. is stable) to better than 1% of central peak out to 10 arcsec radius.	Same calibration accuracy within 20 arcsec	Avoiding confusion from bright sources
	PSF sidelobes are <0.1% at >10 arcsec radius		
Observing modes	Fully-sampled mapping of array field of view. Scan-mapping (areas of square arcmin to square degrees). Single-array mapping.	Hitchhiker mode, with simultaneous sub-mm and optical or infrared observing	
Calibration accuracy	<10% at all wavelengths	<5% at all wavelengths	Relative to standard sub-mm sources, such as planets/asteroids.

5 Detailed Best Effort Calculations of Performance

The performance of the baseline SCOWL design is based on the following assumptions.

Parameter	Value	Notes
Telescope aperture	100m	
Central obscuration	30m	
Primary mirror segment gaps	5mm	Sees warm telescope between gaps. Segment diameter=2m
Secondary mirror segment gaps		Sees warm telescope between gaps
Telescope effective radiation temperature	275K	
Pixel coverage of field of view	35% at all wavelengths	Fraction of science field of view that is covered by Nyquist-sampled pixels
Precipitable water vapour content	0.5mm	See 9.1
Airmass	1.2	Elevation 60 degrees
Atmospheric model		Uses transmission curves from Hitran model, updated 2003
Filter bandwidths	Optimised for atmospheric transmission window	Based on Scuba-2 design
Window losses	4%	Based on Scuba-2. May be thicker, so larger losses for SCOWL
Filter losses	5%	Filters at 1K
Cold stop temperature	1K	
Dichroic losses	5%	Dichroic at 1K. 2 dichroics for 3 wavelengths
Detector NEP	$<3\times10^{-17}$ W/√Hz at 850μm $<1.5\times10^{-17}$ W/√Hz at 450 & 350μm	<1/2 of background power
Detector temperature	100mK	

5.1 Summary of performance

Wavelength	**850μm**	**450μm**	**350μm**	**Units**
Resolution	2.1	1.1	0.9	fwhm, arcsec
System NEFD	0.3	0.6	1.0	mJy/√Hz
Per pixel sensitivity [1] (10σ, 1hr)	50	100	170	μJy
Confusion limit [5]	~1	4	7	μJy
Large-scale mapping sensitivity [2] (10σ, 1hr, 1 sq.degree)	2	5	10	mJy
No. of pixels	10000 [3,4]	20000 [3]	20000 [3]	
Pixel spacing	0.5 [4]	0.5	0.5	Arcsec
Field of view (diameter)	2.5	2.5	2.5	arcmin
Time to map field of view to 10σ=100μJy	0.5	4	17	Hours [3]

1. Sensitivity reached (10σ, μJy) per pixel on the sky (no mapping).
2. Sensitivity (10σ, mJy) reached in a Nyquist-sampled map of 1 square degree in 1 hour (no overheads included).
3. Baseline design using SCUBA-2 type TES arrays. If larger-format arrays are available the number of pixels per band will increase by a factor of ~3-4, and mapping time will be reduced
4. Oversampled at 850μm by a factor of ~2 over Nyquist, in baseline design. Number of pixels at 850μm is effective number of Nyquist-sampled pixels.
5. See section 6.4

6 Comparison to Existing and Proposed Facilities and Space Missions

This section compares SCOWL with other ground and space-based facilities designed to operate over a similar wavelength regime, so which are likely to be doing similar science. The wavelength regime in this comparison is 200-3000μm, i.e. around the Rayleigh-Jeans tail of cool dust at redshifts z<2. Section 6.1 summarises the features of the main instruments and telescopes, including those existing, under construction, and planned for the next decade. In 6.2 & 6.3 the sensitivities are compared in detail, and in 6.5 the complementarity of SCOWL and ALMA is illustrated.
The baseline atmospheric water vapour content for the OWL site in this comparison is 0.5mm. We assume a 100m diameter OWL, with 20000 pixels per short wavelength array. We show in sections 7.2 and 9.1 comparisons of sensitivity with different OWL diameters and PWV, which can be used to scale the other OWL comparisons. The comparisons are based on the parameters in Section 5. The detailed spreadsheet for these is available on request

6.1 Summary of facilities

The following table shows the existing and proposed facilities operating in the submm and far-infrared. The sensitivities are given at the "workhorse" wavelengths.

Telescope /aperture	Instrument	λ (μm)	Pixels	Resolution (arcsec)	Sensitivity (10σ/1hr) (μJy)	Date	Notes
JCMT 15m	Scuba	850 450	37 91	14 7	6000 70000	-2005	
"	Scuba-2	850/450	5100/ 5100	14 7	3000 16000	2006	
IRAM 30m	Mambo-2	1200	117	10	6000	Now	
LMT 50m	Bolocam-2	1100	151	5.5	500	2006	
GBT 100m	PenCam	3000	64	7.5	20		NB: only at longer wavelength
Apex 12m	Laboca	870	295	18	2500	2006?	Also ASTE 10m
"	"C2"	350	300	7.2	13000	2008?	
Herschel 3.5	Spire	500 350 250	1 1 1	35 24 17	5000	2007	
ALMA (500-10000)		850 450 350		0.4 - 0.01 (con-figurable)	170 2500 7000	2012	Also at λ>1mm
Sofia 3.5m	HAWC	200 to 50	384	14" @200μm	30000 (200μm)	2008	Also SPICA
LSD 30m	Large-format camera	850 450 350	20000?	7 4 2	500 800 1000	2012?	Proposed Cornell/ Caltech
OWL 100m	SCOWL	850 450 350	10000 20000 20000	2 1.1 0.9	50 100 170	2015?	

Table 2: Proposed and existing submm facilities

6.2 Per pixel comparison

First we ignore the fact that SCOWL is an array, and look only at the sensitivity of each pixel, assuming an unresolved source.

6.2.1 Flux sensitivity

The charts below compare the pixel sensitivity (NEFD, mJy/√Hz) per pixel for current and planned submm cameras at ~850μm and at 450μm. To convert to sensitivity in 10σ/1hr, divide by 6. Note that we have included in the 850μm comparison the IRAM/30m and LMT/50m values; these operate at 1300 and 1100μm, so the effective sensitivity at 850μm would be a factor of ~2 worse than the values given (assuming some reasonable dust emissivity law). The OWL sensitivity assumes 0.5mm PWV, i.e. a good site; see 9.1)

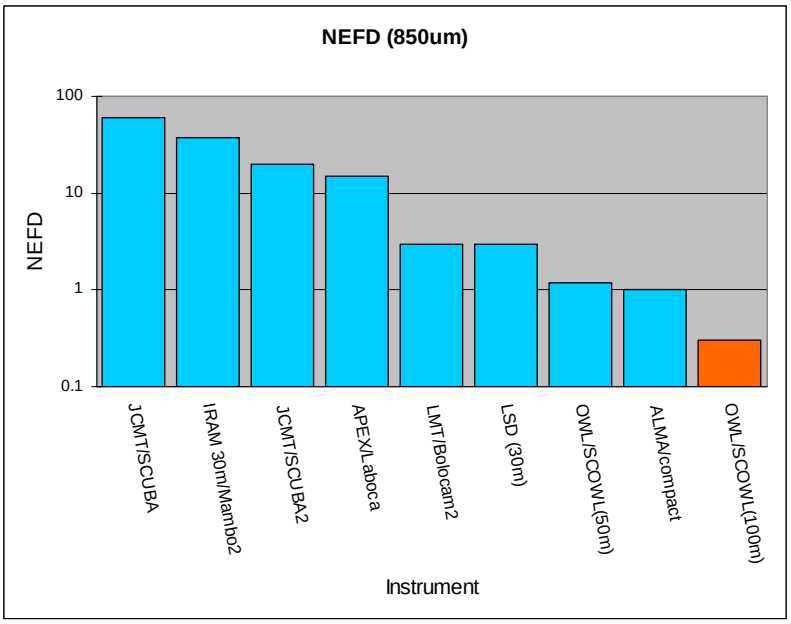

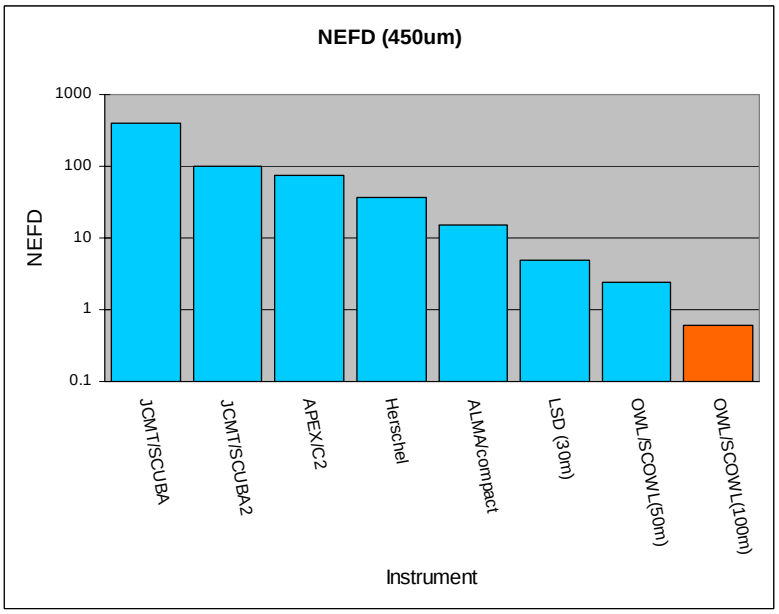

Figure 10 Sensitivity (NEFD) per pixel for various facilities at 850 and 450μm. Note that IRAM/30m and LMT/50m values are those at 1300 and 1100μm. See text for details

The results show that SCOWL on a 100m OWL (shown in orange) will be 3-4 times more sensitive than its' closest rival (ALMA) at 850μm and ~10 times more sensitive than its' closest rival (LSD) at 450μm.

6.2.2 Dust mass sensitivity

Most of the science with SCOWL will be carried out by observing dust. For dust at T>30K at z<2, emission has a spectral index slope of ~2+β, where β=0 (for pure black-body) to 2.0 (for small ISM grains). Taking β=1, Figure 11 shows the relative gain of SCOWL (on 100m shown in orange) for a given *mass* of dust, compared with other facilities. The scale is relative to SCUBA on JCMT at 850μm. Where there are two bars for one instrument, this shows the gains at different wavelengths; in the case of ALMA, LSD and SCOWL the wavelengths shown are 850 and 450μm.

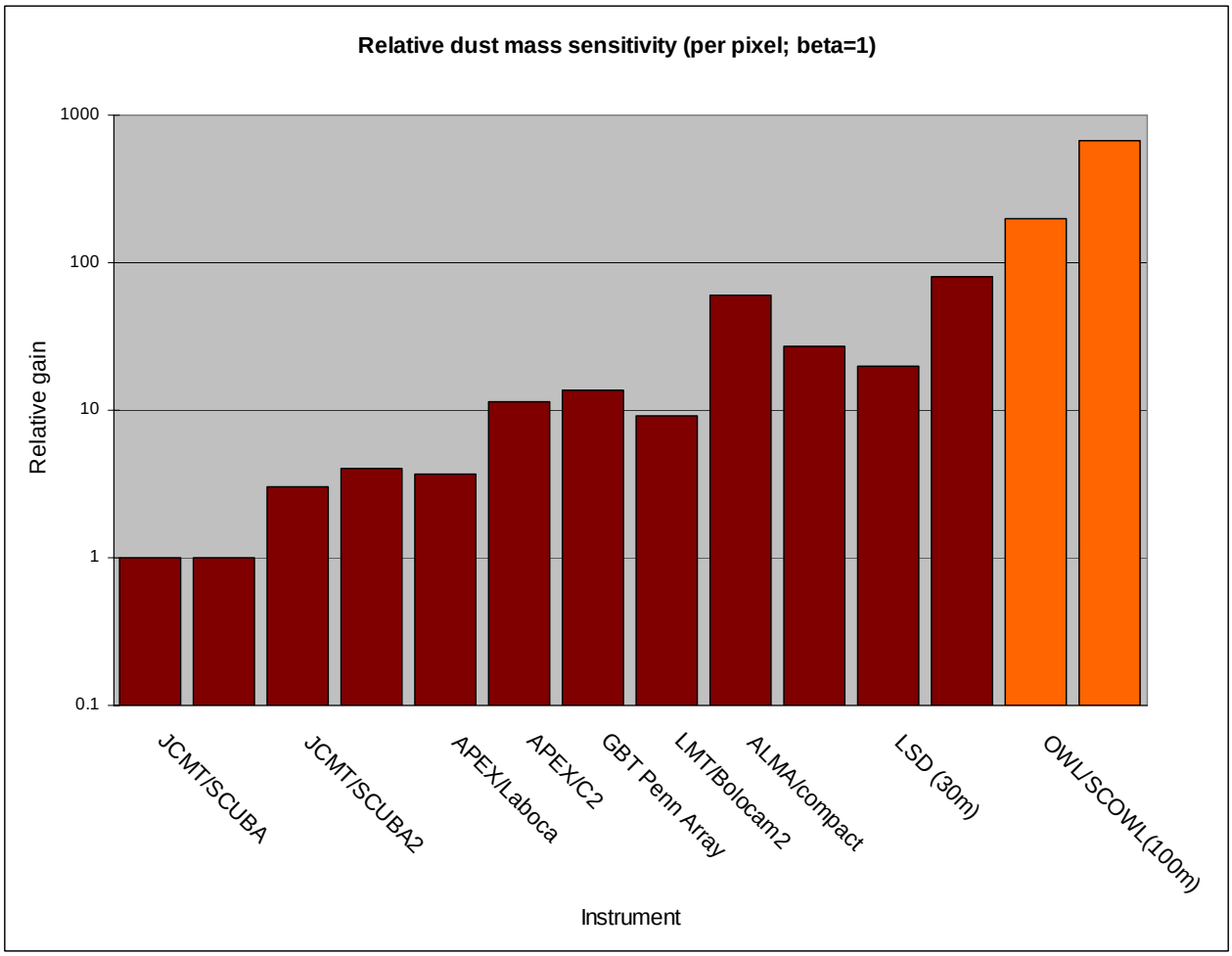

Figure 11: Relative dust mass sensitivity, compared with SCUBA at 850μm.

Figure 11 indicates that SCOWL operating at 450μm on a 100m OWL will be ~700 times more sensitive – *per pixel* - to a given mass of dust compared with SCUBA. Compared with ALMA or LSD, SCOWL will be 10x more sensitive to a given dust mass; this increases to 15x when operating at 350μm. However, these improvements are only realised when SCOWL operates at the shortest wavelength, i.e. 350μm or 450μm. The improvement at 850μm is a factor of ~3 over ALMA. Note that this is per pixel.

6.3 Mapping comparison

The mapping speed, i.e. time to map a fixed area to a certain depth, depends on the number of pixels and beamsize, as well as per pixel sensitivity. Figure 12 below compares the relative mapping speed of various facilities.
Large-scale mapping projects will clearly be more suited to focal-plane arrays such as SCOWL than interferometers like ALMA; the SCOWL mapping speed will be at least 10^6 times faster than mapping with the compact ALMA configuration.

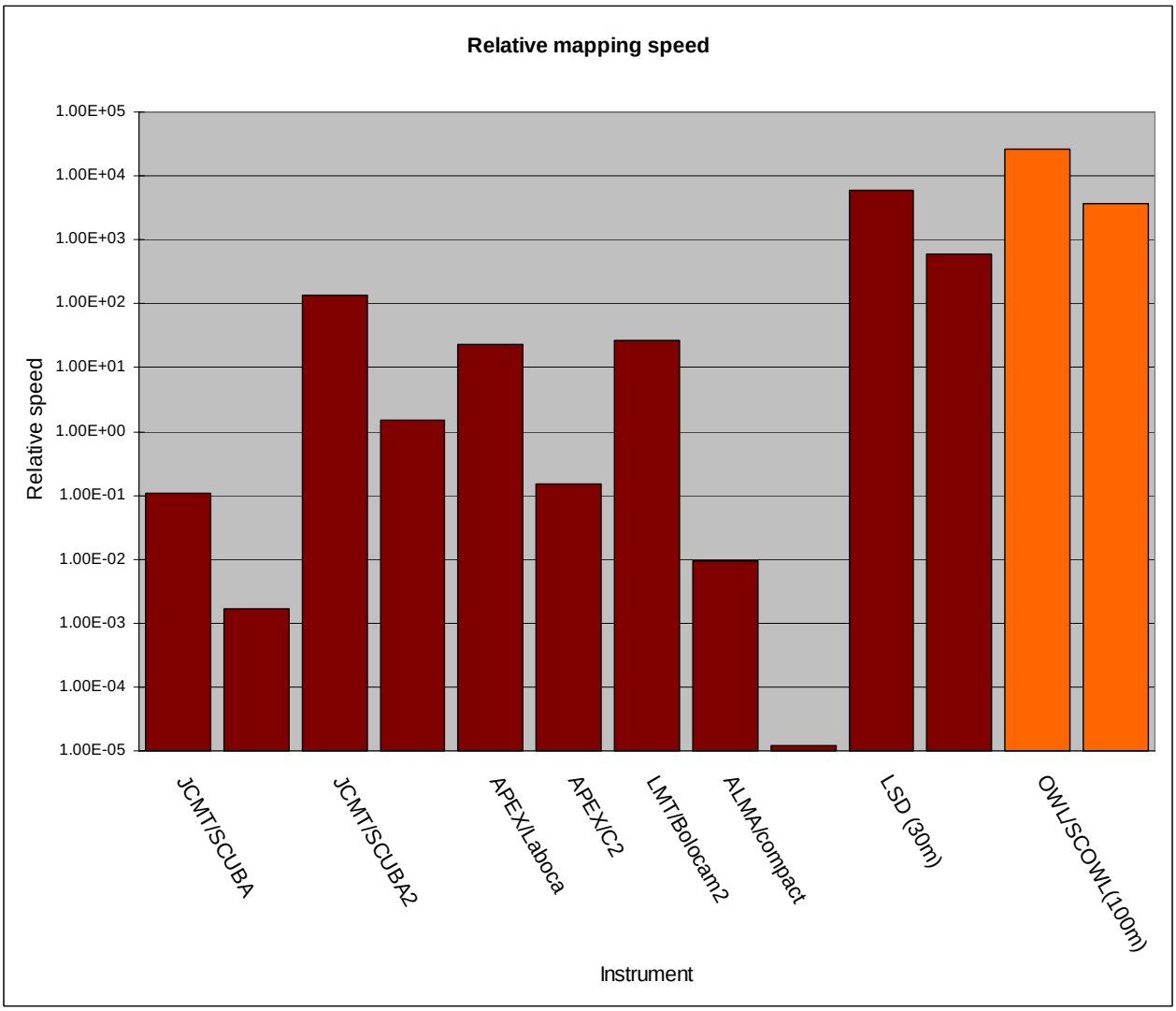

Figure 12: Relative large-scale mapping speed. This shows the relative time for different instruments to map a certain area on the sky to a fixed depth. Large-format focal plane arrays such as SCOWL, as well as telescopes with relatively large beams fare relatively well in this comparison[2]

In summary, SCOWL will be ~2000 times faster in mapping a given area at 450μm compared with SCUBA-2. However, the smaller beam size of SCOWL on a 100m compared with other single-dish telescopes gives it another key capability – a lower confusion limit. This is described in the next section.

[2] The SCUBA-2 and LMT/Bolocam2 score relatively highly in this chart purely because they have relatively low resolution or operate at a longer wavelength (1.1mm) and so are relatively sensitive in mJy units.

6.4 Confusion limits

The sub-mm sky is full of sources. Source confusion for sub-mm and far-infrared telescopes will limit the ultimate point-source sensitivity; in cases where the target source is compact with a known position this can be expressed as the 1σ/1beam sensitivity. For other projects, the number of bright confusing sources over the mapping area will limit the ability to measure, for example, the number density of nearby faint objects in a galactic cluster. Sources of confusion include:

- Solar System Zodiacal dust. This dust is warm (~200K) so is only significant in the mid-IR.
- Galactic cirrus. Cool (~22K) so important in submm. Concentrated towards Galactic Plane.
- Galactic star formation regions. Only dominates in certain regions of the sky.
- High redshift galaxies. Isotropic.

Confusion from high-redshift objects and Galactic cirrus are potentially the most significant problem for the submm. The importance of these is estimated below.

6.4.1 High-redshift objects

The potential problem with the extragalactic background and advantages of smaller beams are illustrated in Figure 13, where models of the confusion limit of SCUBA-2 on JCMT are compared with those of SCOWL.

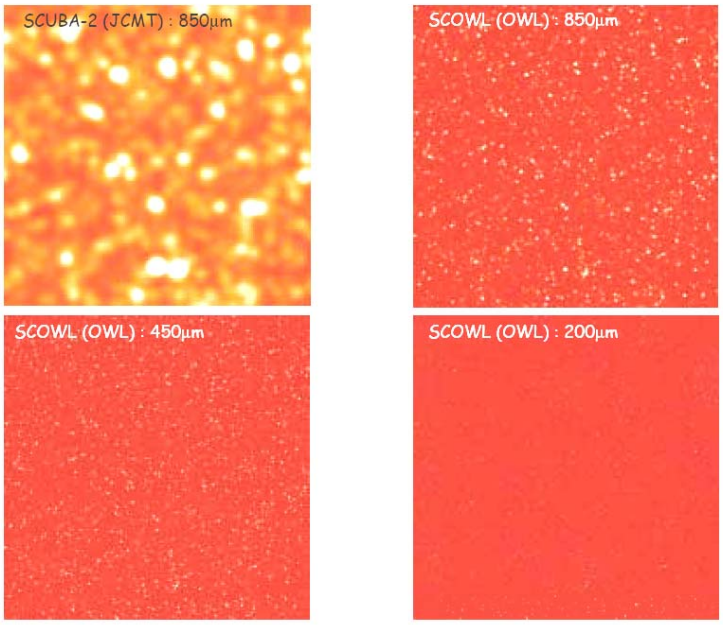

Figure 13: Confusion limited surveys of a 0.1 deg2 area of sky for JCMT/SCUBA-2 at 850μm and OWL/SCOWL at 200, 450 and 850μm. Based on the models of Hughes and Gaztanaga (2000), with simulations carried out by Ed Chapin (details in Chapin et al. 2002).

To estimate the all-sky background confusion limit, we have used the models of Pearson (2001)[3], plotted using a galaxy evolution model. Note that this is extremely uncertain, particularly at the shorter wavelengths, and depends on the populations and evolution of different objects at high redshifts, but recent source counts have not changed the values significantly, and confirmed the 450μm base level (e.g. Greve et al., 2004).
Taking the worst case extrapolation, from this we see that for beam sizes of 2.1 and 1.1 arcsec (fwhm at 850 and 450μm for a 100m OWL) (or 2.7×10^{-7} and 7.3×10^{-8} sq.deg), then this predicts 1σ/1-beam confusion limits of very approximately 0.3μJy at both 850μm and 450μm. The values for different telescope diameters are given in another section (7.2.2).

[3] Available on the web at http://www.ir.isas.jaxa.jp/~cpp/counts/

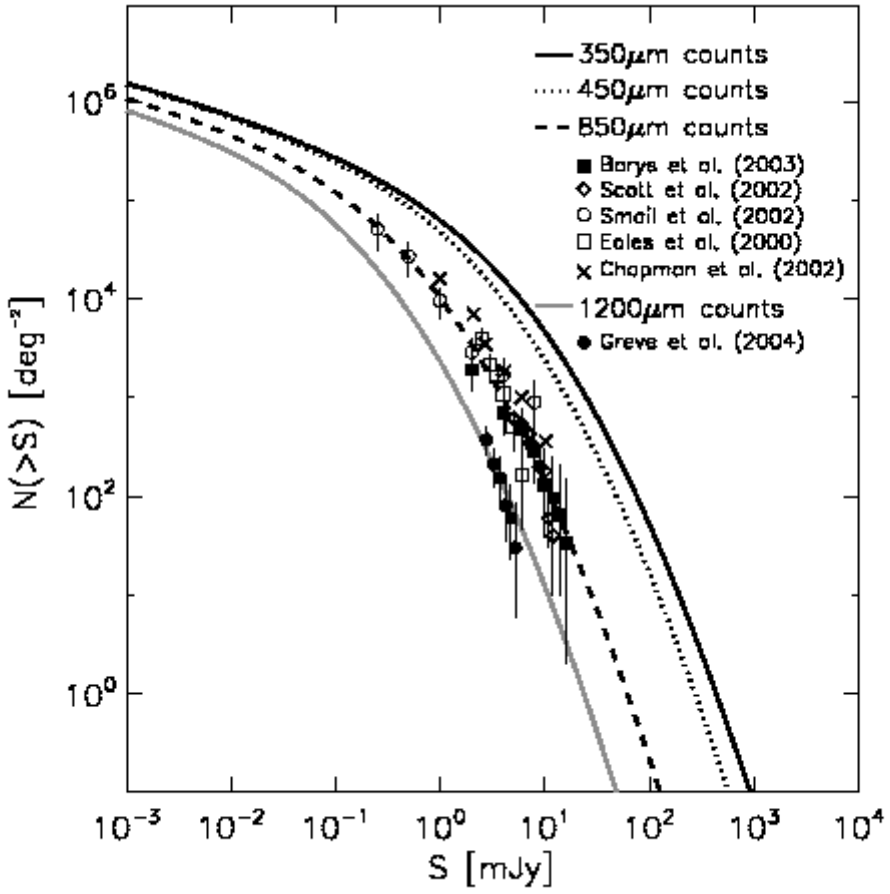

Figure 14: Background number counts at submm and mm (based on models of Pearson (2001) and T. Greve, priv. comm.) The plots have been extrapolated to lower flux densities based on galaxy evolution models, but are extremely uncertain.

6.4.2 Galactic cirrus

This is illustrated by the COBE 240μm map shown in Figure 15. Most of the emission in this figure is cool Galactic rather than hot Zodiacal dust. To estimate the level at longer wavelength we use a mean cirrus temperature of ~22K, with an opacity index 2; this implies the ratio of 240:450 and 240:850 μm fluxes are ~5 and ~40. The fluctuations in background have been measured on the arcsmin scale, not on the 1 arcsec scale. However, if we assume that the approximation for the fluctuations given by Helou & Beichman (1990) are valid down to arcsec scale, then we can derive the confusion levels in the last column of
Table 3. *These numbers are highly uncertain, as the small-scale cirrus structure is unknown. It may be that the power in the small-scale structure is a larger fraction of the background level, which will increase these confusion limits.*

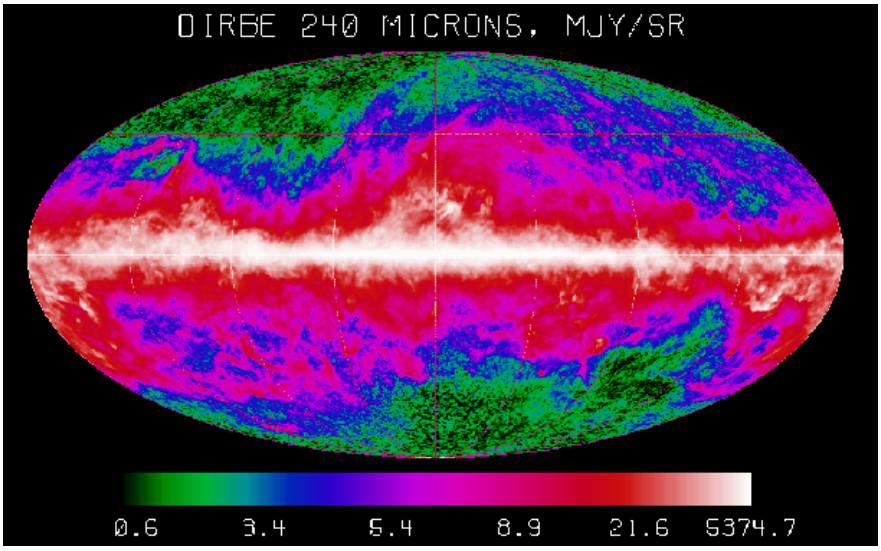

Figure 15. COBE/DIRBE all-sky image at 240μm, showing mainly Galactic cirrus at this wavelength.

Table 3: confusion limits due to Galactic cirrus for different sky coverages. Critical numbers are highlighted.

Wavelength	Fraction of sky not available	Brightness level (MJy/str)	Brightness level (μJy/beam)	Confusion level (μJy)
850μm	1%	1.2	≤100	0.8
850μm	10%	0.07	≤6	0.01
450μm	1%	10	≤230	4
450μm	10%	0.5	≤12	0.05
350μm	1%	22	≤370	7
350μm	10%	1.2	≤20	0.1
240μm	1%	55		
240μm	10%	3		

Note to table: (1) the fraction of the sky at or below a certain brightness level at 240μm is taken from Jeong et al., (2005), converted from their 160μm plot with the dust parameters given above.

6.4.3 Confusion-limited observations with SCOWL.

Confusion affects typical observations in three ways:

- The above 1σ/1beam confusion limits sets the lowest achievable noise level in a map. It is the lowest flux detectable for a point source of known position. This is given in Table 4.
- An alternative way of expressing the confusion limit sometimes used is 1/30 sources per beam. (eg Takeuchi & Ishii, 2004). So we require that a field of view of 30 beams has no more than 1 significant detection, at ≥5σ. This is arbitrary, but would result in the detected confusing sources being ~5 beams separated. This is given in Table 5. For the 850μm beam this is roughly equal to 1 per 100 sq.arcsec. This limit is more appropriate to small-scale mapping.
- For large-scale mapping of point sources, the statistical uncertainty in number of background objects (nominally √N, but probably a factor of ~2-3 higher[4] because of background clustering and lensing) sets a limit to the measurable number density of foreground objects. The number density of objects is given in Table 6 for a 1 degree field mapped in 1 hour.

[4] Rough estimate, depending on mapping area compared with typical cluster size and enhancement, and lensing effects. Neither of these is currently well known.

Other methods of differentiating against background sources can be employed:

- Multi-colour imaging, looking at differences in the 350/450/850μm relative fluxes between different classes of objects.
- Proper motion of the foreground objects. This would be useful in nearby stars, within ~20pc, and so would be useful for example in detecting faint clumps in nearby debris discs.
- For large-scale mapping of extended emission, it will be possible to remove bright background *point* sources using post processing. However, it is likely that some background Galaxies will be extended. These may be mostly the more luminous and less common ones.

The definition of a confusion limited observation depends on the project. *A reasonable limit for point source detection is to reach a noise level of 3x the confusion limit.* This sets the limit of observing time on one point in the sky. The confusion limits for different types of projects using SCOWL on a 100m telescope are given in the following tables. The corresponding values for different telescope diameters are given in section 7.2.1.

Table 4: summary of point-source confusion limits for SCOWL.

	850μm	**450μm**	**350μm**
1σ/1beam confusion limit: **99% sky coverage** **[90% coverage]**	~1 μJy [~0.3]	≤4 μJy [≤1]	≤7 μJy [≤1]
Time to 3x confusion limit (for point source): **99% sky coverage** **[90% coverage]**	3 hrs [30 hrs]	≥1 hr [≥11 hrs]	≥1 hr [≥30 hrs]

Table 5: summary of nearby-source confusion limits for SCOWL.

	850μm	**450μm**	**350μm**
5σ/30 beams confusion limit: **(for ~1 background object in 30 beams, at 5σ detection)**	1σ=12μJy	1σ=6μJy	1σ=2μJy
Time to map FoV to confusion limit	1 hr	10 hr	400 hrs

Table 6: summary of extended-mapping source counts for SCOWL.

	850μm	**450μm**	**350μm**
10σ/1hr 1 sq. degree, number of sources N:	3000	8000	6000
Mean source separation (arcsec)	60	40	47

6.5 SCOWL and ALMA

The premier facility for *high-resolution* millimetre astronomy in the next decade will clearly be ALMA. Yet a 100m OWL offers the opportunity to observe with a similar geometric collecting area to ALMA, but with a near perfect dish surface accuracy and a single aperture. Thus the *effective* collecting area of OWL, observing at the short submillimetre wavelengths, will be approximately twice that of ALMA. A wideband bolometer array such as SCOWL will provide a facility which would surpass ALMA in several respects. The larger effective collecting area combined with the wider bandwidth of such a bolometer system will mean a factor of ~10 improvement (or x20 at 350μm) in point-source sensitivity to a given mass of dust (see table below). However, with the proposed large-format focal plane array of SCOWL, the most significant gain will be in large-scale mapping speed. Table 7 indicates that projects to make extremely deep maps of *square degrees* of sky now become feasible with SCOWL; we give the time to map 1 square degree to a 10σ sensitivity of 0.1mJy. For comparison, the long-term SCUBA-2 legacy large-area survey is going to map several square degrees to 10σ=7mJy over the next 4-6 years (but with a 14 arcsec beam). Clearly this sort of project would not be possible with ALMA.

	SCOWL (100m)		**ALMA**	
	850μm	450μm	850μm	450μm
Flux sensitivity (μJy, 10σ 1hr)	**50**	**100**	170	2500
Relative dust mass sensitivity (cf SCUBA-2)	**70**	**220**	20	9
Resolution (arcsec)	2.1	1.1	**0.02**	**0.01**
Confusion limit (μJy)	~1	4	**<0.4** [5]	**<0.02**
Mapping speed (time per square degree to 10σ=0.1mJy)	**30 nights** [6]	**200 nights**	200,000yr	200Myr

Table 7: SCOWL and ALMA capabilities. Areas where the facility is optimally suited are indicated in red bold.

[5] Worst case, for compact configuration
[6] assuming 12-hour nights

7 Scope of the Ideal Instrument

7.1 Modes

A brief outline of the main data-taking modes is as follows.

Record flat-field illumination – a source of radiation is inserted in the beam to provide uniform illumination to the arrays and to provide the basis for calibrating the bolometers relative to one another.

Calibration with dark shutter closed – the cold dark shutter is closed isolating the bolometers from all radiative power input. Measurements are then taken at various setting of the pixel heaters to determine the response curves of the bolometers.

Atmospheric extinction calibration – measurements are taken of the flux from the sky at a range of zenith angles in order to separate the Earth's atmospheric emission from telescope emission. This allows the Earth's atmospheric emission to be determined directly from science frames, and the atmospheric extinction can then be calculated.

Mosaic map – a series of CCD-style exposures of the science field are taken interspersed with adjustments to the telescope position to make a mosaic which fills-in the gaps between the subarrays.

Scan map – data frames are recorded continuously at 200 frames/sec while scanning the telescope over the science area.

Telescope pointing - check and adjust telescope pointing by imaging a bright point source on one of the subarrays.

Telescope focus - check and adjust telescope focussing by imaging a bright point source on one of the subarrays.

Mosaic map polarimetry – a polarimeter version of mosaic map. The half-wave plate is spun at about two revolutions per second, resulting in the polarised signal being modulated at 8Hz.

Scan map polarimetry – a polarimeter version of scan map.

7.2 Advantages of 100m cf other primary diameters

7.2.1 Comparison of sensitivity with different telescope diameters

The two primary *telescope* parameters which will have a direct effect on the SCOWL sensitivity are the primary diameter and the atmospheric precipitable water vapour content (PWV – see Section 9.1). The following shows the effect of primary diameter on the NEFD. This scales the above sensitivity comparison charts.

Note that the atmospheric values shown are at elevation 60^{o} (Airmass 1.2). Observing at an airmass of 2.0 is approximately equivalent to doubling the PWV.

	Diameter	NEFD 850μm	NEFD 450μm	NEFD 350μm
(assuming PWV=0.5mm)	100m	0.31	0.66	1.1
	50m	1.2	2.6	4.4
	30m	3.4	7.3	12.2

On this table, red indicates the NEFD is more than a factor 3 worse than nominal

7.2.2 Comparison of confusion limit with different telescope diameters

The table below gives the confusion limits and time to reach that sensitivity for SCOWL at 850 and 450μm with 3 different telescope diameters. At low flux levels (tens of μJy – see section 6.4) the confusion flux level from high-redshift background galaxies depends on the beam area $A^{-2.5}$, or telescope diameter $D^{-4.5}$, whereas cirrus confusion depends on $D^{-2.5}$. The background number counts turn over around 1mJy. We have assumed that 99% of sky coverage is required (giving the larger confusion limits at 350 and 450μm). The final row gives the confusion limit on the JCMT, with SCUBA-2 sensitivities.

Table 8: confusion limits for SCOWL with various telescope apertures.

Telescope diameter (m)	Beam area (square arcsec)		Confusion limit (1σ 1-beam, μJy)		Time to confusion limit		Sensitivity (μJy)	
	850μm	450μm	850μm	450μm	850μm	450μm	850 μm	450 μm
100	3.5	1	1	4	3 hrs	≥1hrs	50	100
50	14	4	12	23	3 hrs	≥3hrs	200	400
30	39	11	150	130	1 hr	≥0.5hrs	500	850
15 (JCMT)	154	44	400	800	50 hrs	400 hrs	3000	16000

7.2.3 Overall comparison with a smaller aperture telescope

Going from a 100m to a ~50m telescope has the major disadvantage of a loss of ~4 in sensitivity (or a factor ~20 longer in integration time). Also, possibly more significantly, the confusion limit is a factor of ~10 worse with the 50m dish.

7.3 Study with incomplete M1

SCOWL could be operated with an incomplete M1, *but only if the segments were populated from the centre out*. A random or other pattern of segments would mean the detectors were looking at warm background (at ~280K), and the performance would deteriorate significantly.
The size of the cold stop could be changed incrementally to reflect significant changes in the size of the useful primary diameter as M1 is populated outwards.

8 Background to Observing Modes

The various observing modes suggested for SCOWL are being developed for SCUBA-2 and will be tested when that instrument is delivered.

8.1 Field Rotation

The OWL telescope design includes turntable mounts for the instruments to allow compensation for field rotation. The current SCOWL proposal exceeds the mass limit of the turntables, and so this description assumes no field rotator and the instrument is assumed to be fixed relative to the telescope. The astronomical image therefore rotates relative to the instrument focal plane. This is handled by taking images rapidly and correcting for field orientation in software, which is the approach used at JCMT. The detectors are non-integrating devices and so acquiring data with a high frame rate is unavoidable even in the absence of field rotation.

The addition of a turntable suitable for SCOWL would have some advantages (mosaic and scan patterns would not need to rotate relative to the astronomical image) but this is not a major issue.

8.2 Mosaic Maps

The physical construction and mounting of the subarrays leaves large gaps in the coverage of the focal plane. The most straightforward way to overcome this is to fill-in the gaps by taking a series of data frames at various telescope offsets. The data frames have to be corrected for pixel-to-pixel electrical zero point drifts by reference to a recent dark measurement. This requires the zero point drifts to be smaller than the photon noise averaged over the interval between dark frames. The feasibility of this mode clearly depends upon the array stability, which is a factor yet to be determined as part of the SCUBA-2 project.

8.3 Scan Maps

The scan map technique, whereby data frames are acquired rapidly while the telescope scans over the science area, is useful both as an alternative way of filling the gaps between subarrays and as a method for making maps of areas larger than the focal plane. The technique is heavily dependent upon having a suitable map reconstruction algorithm. The method results in any sky pixel being measured by multiple bolometers, and this can be used to determine the relative bolometer zero points independently of taking dark frames.

A key factor is the pattern of scanning used, and the ability to tag each of the 200 frames recorded per second with the corresponding telescope position. Astronomers using the SHARC-II instrument have studied various scanning patterns, and have concluded that, for smallish maps, Lissajous figures have good properties with respect to avoiding excess telescope accelerations (in general telescope position uncertainties become unacceptable at high accelerations).

Alternative scanning strategies and matching image reconstruction techniques are being studied for SCUBA-2, making careful use of the advances made by the SHARC-II team.

8.4 Polarimetry

It is expected that successful polarimetry will require spinning the half-wave plate at a sufficient speed that 1/f noise due to the Earth's atmosphere is significantly below photon noise. In the sub-mm, measurements at 8Hz are expected to be sufficient, which means spinning the half-wave plate at two revolutions per second. A dominating feature of the raw data will be the polarising effect of the telescope optics on the sky background, which will produce a linearly polarised signal many orders of magnitude brighter than the required science signal. Handling this requires accurate relative calibration of the bolometers.

For SCUBA-2, people are also considering the possibility of a scan map mode for making polarisation maps of extended sources. The feasibility of this is speculative at present.

9 Study of Observatory Requirements

9.1 Site and PWV

The atmospheric precipitable water vapour content has a strong and significant effect on the SCOWL sensitivity, as shown in the following table.
Note that the sensitivity values shown are at elevation 60° (Airmass 1.2). Observing at an airmass of 2.0 is approximately equivalent to doubling the PWV from Zenith.

PWV content (mm)	Optical depth at zenith at 225GHz	NEFD 850µm	NEFD 450µm	NEFD 350µm
0.5mm	τ_{225}=0.03	0.31	0.66	1.1
1mm	τ_{225}=0.06	0.36	1.4	2.5
2mm	τ_{225}=0.1	0.49	6.1	12
4mm	τ_{225}=0.19	0.9	117	285

On this table, yellow indicates the NEFD is a factor 2 or worse than nominal and red is more than a factor 3 worse.

There are often significant diurnal, seasonal, and longer-term (e.g. El Nino) effects – often a factor of 2 in PWV; some sites are more variable than others. But very roughly, the following sites give a reasonable fraction (up to ~50%) of time where the PWV is equal to (or better than) the value indicated. *At this stage the values are a very rough guide; different authors give different answers, and the variations are large.*

PWV *	"Typical" site	Reference
0.35mm ±0.2	Antarctica (3000m)	http://astro.uchicago.edu/cara/research/site_testing/submm.html
1.2mm ±0.5	Atacama (5000m)	http://alma.sc.eso.org/htmls/sumary9899.html
1.8mm ±1	Mauna Kea (4200m)	http://puuoo.caltech.edu/tau_plot.html
~3mm	Paranal (2500m)	http://www.eso.org/paranal/site/paranal-figs.html#water
~4mm	Pico Veleta (3400m)	http://iram.fr/IRAMES/otherDocuments/manuals/manual_v20.ps

* Note: the PWV is the range of the 25 and 50% quartiles, averaged over Winter and Summer.

9.2 Seeing and AO requirements

The AO requirements for SCOWL and for the mid-infrared instrument (TOWL) have been outlined in RD05.
The variations in the position and "Strehl ratio" of a telescope beam at submm wavelengths are dominated by variations in the PWV content over different parts of the aperture. This is most evident with submm interferometers such as the SMA (and eventually ALMA), where corrections for varying water vapour content are being made for each element independently, and used to make corrections in the final cross correlation. A study of the effects on the SMA has been made and is described in http://sma-www.cfa.harvard.edu/memos/tech_no.html Memo 154. Table 7 compares the submm seeing (under median conditions for the SMA) with the SCOWL resolution. The so-called

"anomalous seeing" effects occur when the atmosphere is more unstable, generally at Sunrise and Sunset; they can be several arcsec, even on good sites.

The timescales for the submm seeing variations are set by the time for water-vapour clumps to cross the aperture (in the near field). For winds of 20km/hr (5m/s) this would be ~20 seconds.

Table 9: Submm seeing (based on SMA Memo 154)

Wavelength	**Submm seeing (for median conditions on Mauna Kea)**	**Submm seeing (poor conditions, Sunrise/Sunset)**	**SCOWL diffraction limited beam**
850μm	0.9"	~10"	2.1
450μm	1.1"	~10"	1.1
350μm	1.2"	~10"	0.9

9.2.1 Submm seeing measurement and correction

The water vapour variations do not affect the optical (to 1st order), so submm seeing measurements cannot be made with optical guide stars. However SCOWL could employ the same technique as used by interferometers, by measuring the atmospheric emission at different points over the aperture, and correcting the telescope tip/tilt or low-order AO corrections. This is the "Water-vapour-AO" system mentioned in RD05.

9.2.1.1 Tip/tilt corrections

Corrections would have to be made on a 20-second timescale. This could be done by moving the telescope (tip/tilt), or feeding the information to the DR system, for corrections in the regridding algorithm. The latter software correction would be acceptable. Four water-vapour monitors could be used at the edges of the aperture – or two differential ones for each axis.

9.2.1.2 AO corrections

This could only be done using the primary or secondary actuators, in a low-speed (0.1-1Hz) high-amplitude (1-10 arcsec) mode. It would require multiple water-vapour monitors over the aperture.

9.2.1.3 Submm guide stars

The submm number count suggests that over a 2.5 arcmin fov, there will be a few 1-3mJy background galaxies. These may be point sources, or contain a significant compact component, and the sensitivity is such that the s:n will be ~10σ on these in ~1 second. Thus they could be used as "guide stars" for shift-and-add, to remove both flexure and submm seeing. This is dependent on the exact background number count model and their size distribution, but these confusing sources may be put to good use. Cross-correlation of the whole-field structure in individual frames might be the most sensitive way of doing this measurement, as it takes advantage of all the lower-level background structure. This would need to be investigated.

9.3 Additional telescope requirements

9.3.1 Telescope velocity and acceleration

An additional telescope requirement for SCOWL operation in the scan mapping mode is that the telescope sky coordinates should be available in real time, at a 200Hz rate. This is to allow the telescope to be scanned over the sky,

in some defined but potentially complex motion, whilst taking data continuously and regridding into the final image. See section 8.3.
The data rate for efficient sky removal is 200 frames/second. The required telescope velocity and acceleration are given in the following table.

Table 10: requirements on telescope velocity and acceleration

	Requirement	**Goal**	**Notes**
Telescope scan velocity	50 arcsec/second		For scan mapping
Telescope acceleration	100 arcsec/second^2		For high efficiency, scan using Lissajous figures

Note that the observing modes planned for SCOWL (and SCUBA-2) do not require any chopping or nodding of the telescope.

9.3.2 Daytime observing

Unlike optical and the near infrared, submm observing can frequently take place efficiently during the day. The main astronomical limitation is the atmospheric stability. On Mauna Kea, the sky is stable enough to allow daytime observing time to continue to 9 or 10am local time, and on exceptional days, observing can continue all day. Thus OWL would be utilised more efficiently, potentially resulting in 10-30% more observing time and scientific output from the observatory. However, this operation places several requirements on the telescope and observatory:

- The alignment of the individual telescope segments must be maintained to the desired accuracy (to maintain <<1 arcsec beam size) without the use of guide stars. Possibly this could use a lookup table although the effects of wind would need to be considered.
- Careful sun avoidance systems would obviously be required. This would not only be for the primary and secondary, but also all the concave mirrors. The effect of solar heating on the telescope structure would need to be investigated.
- Fast and efficient switchover to daytime/sub-mm observing is needed.

9.3.3 Instrument data rate

From the SCUBA-2 studies, a frame rate of 200Hz is required for the TES detector readout. Some data compression is possible, to reach ~3 byte words. For example, for 3 arrays each of 20,000 pixels, the total data rate from SCOWL will be 20000 x 3 x 200 x 3bytes, = 50Mbytes/second, or 2Tbyte/night. This is a sustained rate, as most observing requires scanning and fast readout.

10 Instrument Conceptual Design

10.1 SCUBA-2 as a SCOWL prototype

The baseline design of SCOWL presented here is based on the SCUBA-2 concept. So SCUBA-2 can be regarded as a "prototype" for SCOWL; this has the advantage that several of the high-risk areas will be tested once SCUBA-2 has been commissioned and is running reliably on the JCMT (likely to be ~2007-2008). Areas where we would expect particularly useful feedback for the SCOWL project are the TES detector arrays and readout, calibration method, observing techniques, cooling system, and overall design. Areas where SCOWL will be significantly different would be the Cassegrain mounting (SCUBA-2 is Nasmyth-mounted), the higher pixel count and wire count, heavier heat load, and possibly the use of different detectors arrays.

10.2 Optics

10.2.1 Optical concept

The optical concept of OWL is based on a all-reflective optical design using the F/6, 100-m telescope OWL as the input to the instrument. There are 2 warm mirrors N1 and N2 producing a beam entering the cryostat through a window and a cold stop at 4K. The cold mirror N3 relays the F/6 telescope focus to the F/4 beam on the detector. In the present optical design only 1 cold stop at 4K has been provided so we need to make sure that the detector at 1K is properly baffled and the thermal background due the 4K cold stop properly filtered. Introducing a 2nd cold stop in the system will complicate the optical design and increase the size of the instrument.

10.2.2 Specification:

- Telescope: OWL diameter: 100-m
  F/6
  plate scale: 2.91 mm/arcsec
  for a FOV of 2.5 arcmin the focal plane is 437-mm
- SCOWL: wavelength range: 350- 450 and 850 μm
  FOV: 2.5 arcmin
  F/4: scale: 1.94 mm/arcsec
  2 pixels of 1-mm each/arcsec
  detector diameter: 291-mm
  accommodate 4 SCUBA-2 modules, of 4 chips each, per waveband

10.2.3 Optical layout

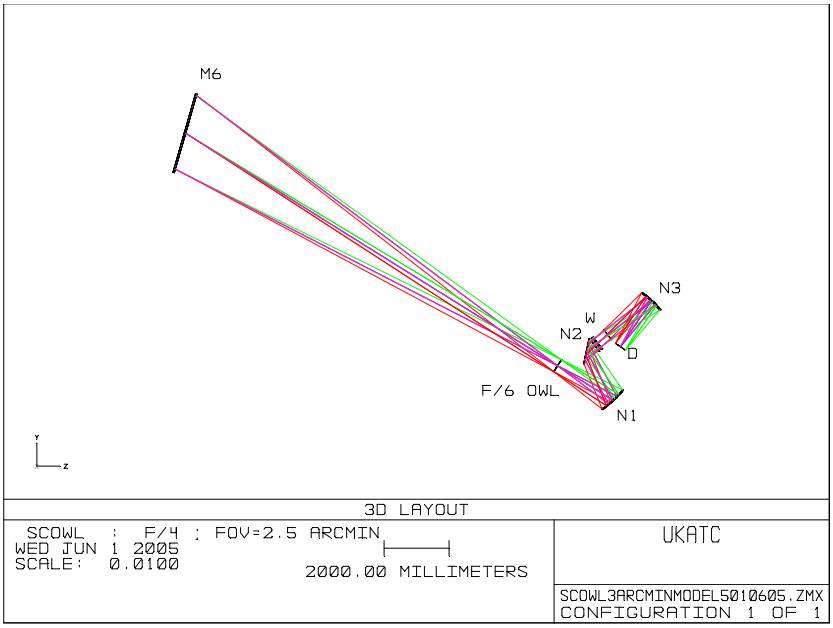

Figure 16: Optical layout SCOWL

10.2.4 Optical data:

The following table summarises the optical data in the design. The biconic Al mirrors are manufacturable with the present technology used on SCUBA-2 mirrors, the window and the filters are under study concerning their manufacturability. The current max size for the filters is around 200-mm.

OPTICS	Radius mm	Separation mm	Material	CA mm
FP OWL F/6	Plano	2000	Air	437
N1	4101.43	1700	Al Biconic mirror	870
N2	Plano	300	Al Flat mirror	795
WINDOW	Plano		HDPE_300	470
FILTERS	Plano		HDPE_300	455
COLD STOP	Plano	2100	Air	400
N3	3037.32	1700	Al Biconic mirror	766
FILTER	Plano		HDPE_300	400
IMAGE	Plano			383

Table 11: Optical data of SCOWL

10.2.5 Strehl ratio

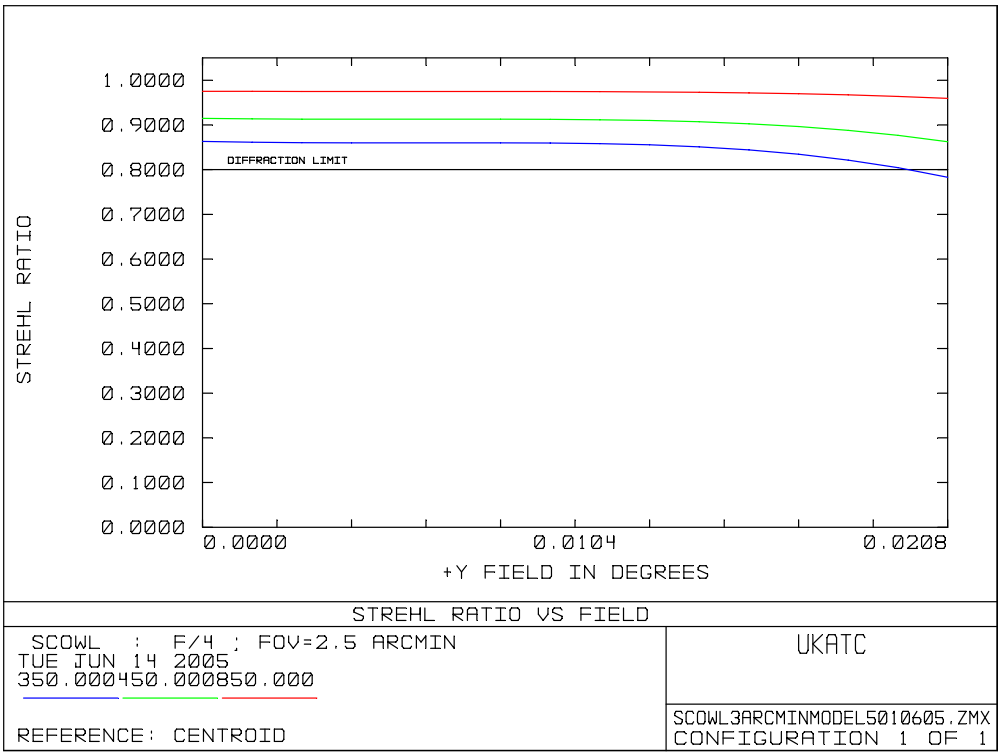

Figure 17: Strehl ratio as a function of FoV for 350, 450 and 850 µm

10.2.6 Spot diagrams

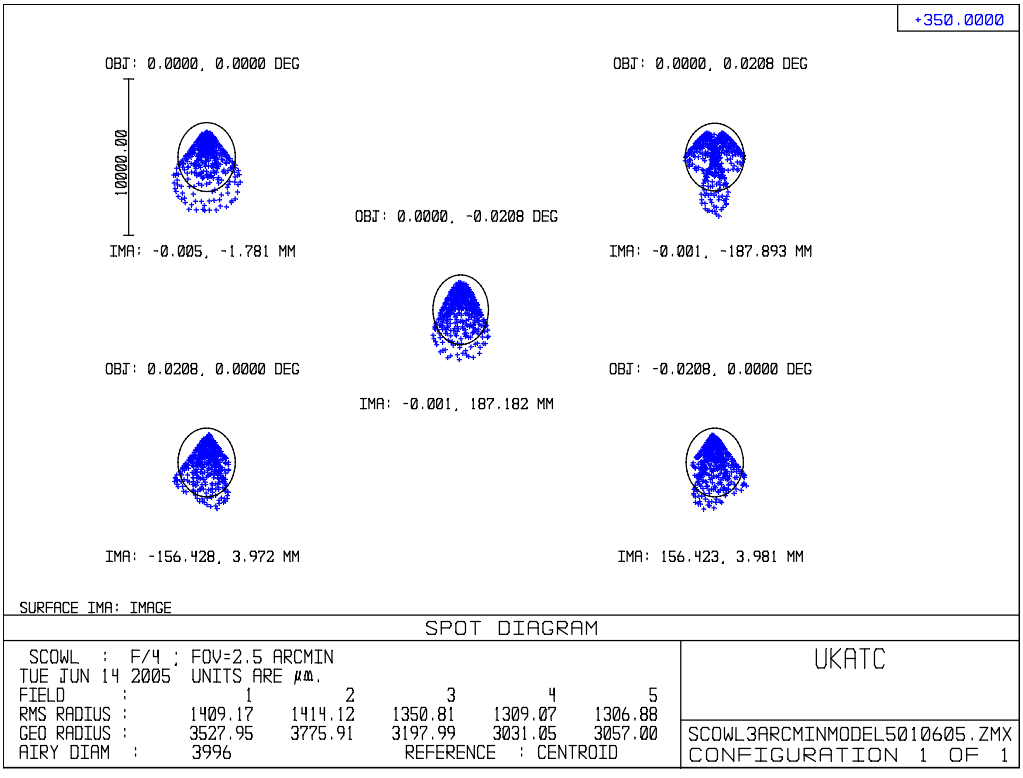

Figure 18: SCOWL Spot diagrams at 350 µm

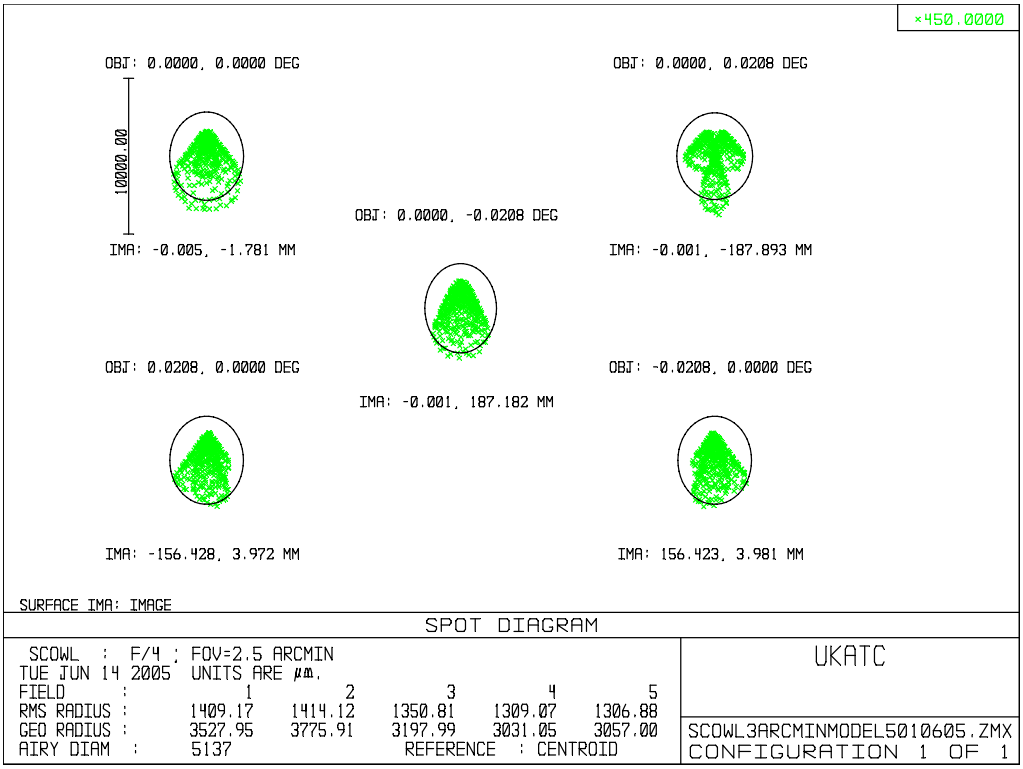

Figure 19: SCOWL spot diagrams at 450 µm

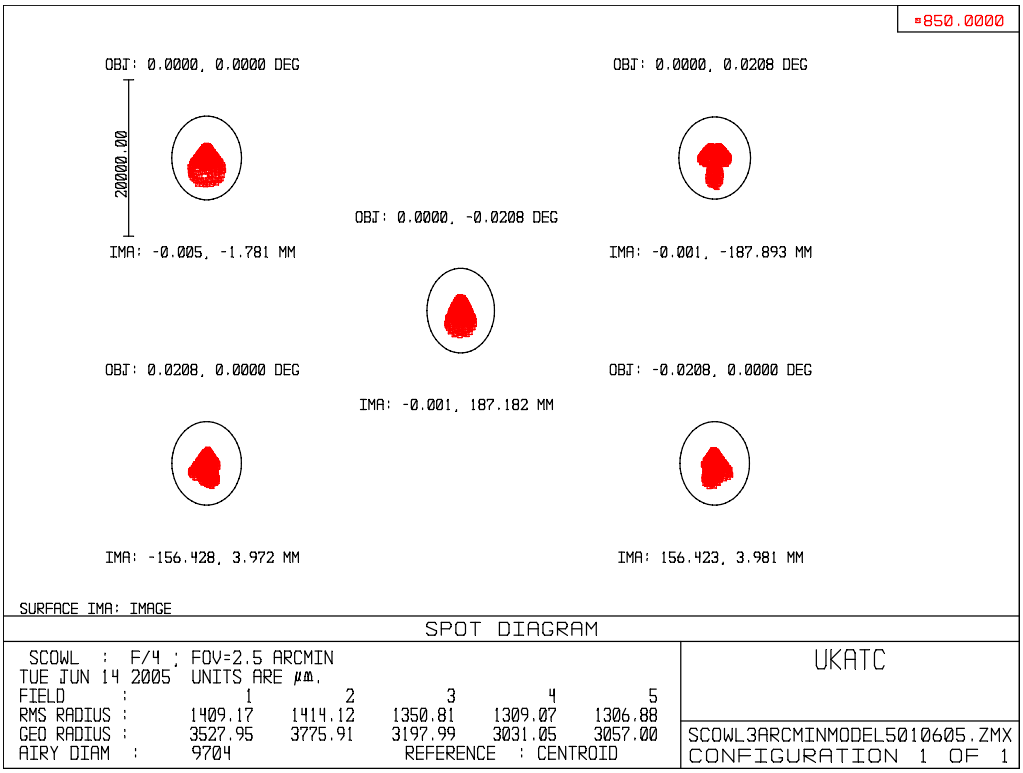

Figure 20: SCOWL spot diagrams at 850 µm

The Airy disk (defined by 2.44 λF) is shown around the spot diagrams. Spots are inside the Airy disks which means that the optical design will give diffraction limited images. Coma and astigmatism are the dominant geometrical aberrations and could be compensated by the active telescope to improve the image quality.

10.2.7 Conclusion:

The SCOWL preliminary optical concept meets the image quality requirement (diffraction ltd system for the working wavelength) for most of the 2.5 arcmin FoV. The manufacturability of the window and filters still remains an issue. A number of options which may optimise the design even further include investigating the use of:

- 2 cold stops at 4K and at 1K
- Nyquist sampling for all the 3 channels, meaning that if we have only 1 type of detector size, say 1-mm pixel, we will need to have 3 different F-numbers and 3 imaging mirrors N3.

Wavelength (μm)	350	450	850
F	2.35	4	5.7

- Position and number of dichroics
- Position of waveplates for polarimetry
- Position and number of filters

10.3 Mechanical

The SCOWL mechanical design has been developed according to the ICD document ref AD02 and further modified according to the Adaptor-Rotator concept document RD03.

10.3.1 Cryostat description

The SCOWL cryostat concept (Figure 21) is based on the SCUBA-2 design and has 4 temperature stages (60K, 4K, 1K and ~100mK). These are isolated from each other using trusses made from G10 for the 60K and 4K stages and Carbon fibre for the 1K stage. Sapphire isolation stages are used to mount the mK systems within the FPUs. Four pairs of trusses are used for each stage. The 60K and 4K stages form complete radiation shields around the colder stages in order to minimise stray light and thermal loads. The 1K FPUs are individually fixed to the 4K structure (truss structure not shown).The cryogenic stages are permanently attached to the vacuum vessel lid. Access to the cold stages is achieved by removing the lower sections of the vessel, 60K shield and 4K structure. The central section of the vessel and the attached warm electronics can remain in position in order to minimise disruption to the array wiring. Construction of the SCUBA-2 cryostat is nearing completion and it has been successfully cooled to 4K. The dilution Refrigerator (DRF) is currently undergoing commissioning at the UK ATC prior to installation in the cryostat and the optics have all been manufactured and installed. The following table gives a comparison between the SCOWL and SCUBA-2 instruments.

Table 12: Comparison of SCOWL and SCUBA-2 cryostat requirements

	SCUBA-2	**SCOWL**
Volume	5.0m^3	Ø2.26m x 2.4m = 9.5m^3
300K Surface area	12.5m^2	24m^2
Window aperture	0.11m^2	0.31m^2
Wire count	3560	21360

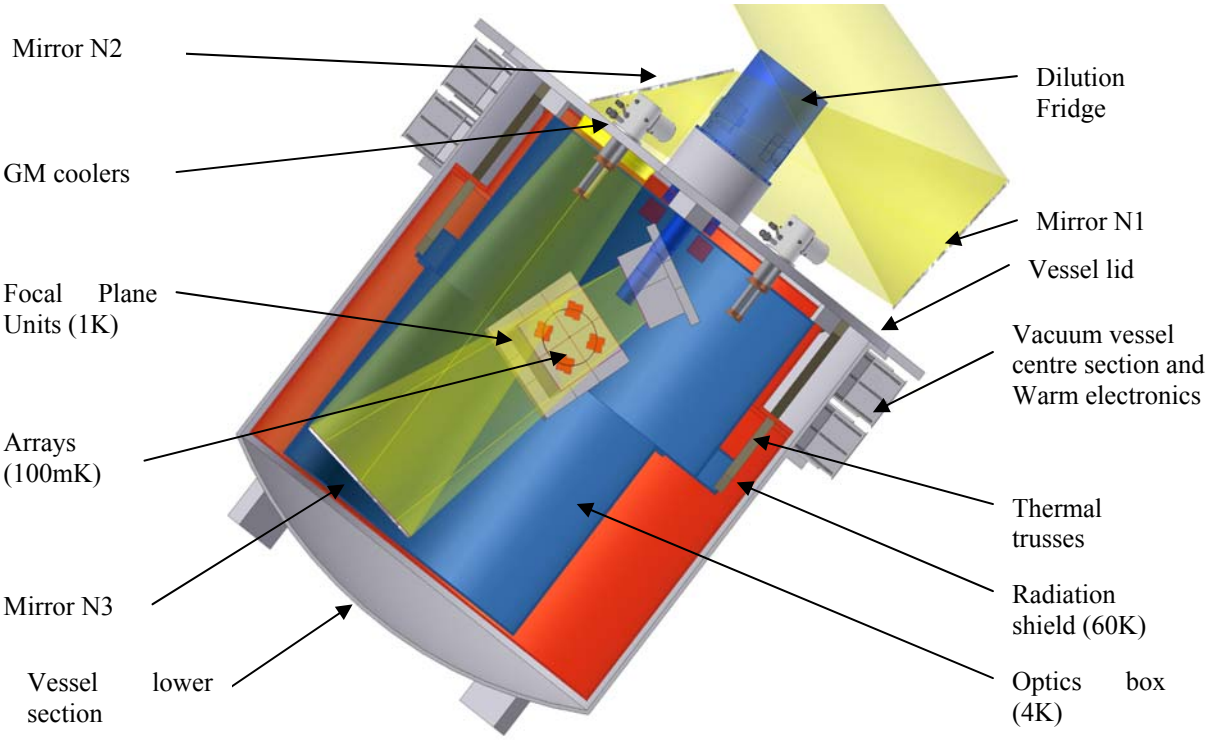

Figure 21: Section through the cryostat concept

10.3.2 Optics

10.3.2.1 Cold stop

In SCUBA-2 the cold stop is cooled to 1K. In SCOWL the cold stop is at 4K. Further work would be required to determine if this produces an acceptable background at the array. There will be a 1K field stop in front of the arrays.

10.3.2.2 Mirrors

There are 3 mirrors in the SCOWL design as follows:

N1 870.82mm Diameter
N2 795.15 mm Diameter
N3 766.22 mm Diameter

Of these only N3 is cryogenic, and will be cooled to less than 15K to minimise the thermal background. All of these mirrors are smaller than the mirrors which have already been manufactured for SCUBA-2, the largest of which measures 1080 x 1020mm. The mirror surfaces are either biconics or flats, which are also easier to manufacture than the SCUBA-2 free-form surfaces.

10.3.2.3 Window

SCUBA-2 uses a planar window with a 200mm Clear Aperture (CA), which is made from 8mm thick Ultra High Molecular Weight Polyethylene (UHMW PE), which produces a loss of 10% and has a factor of safety on failure of ~2. The window for SCOWL has a CA of 471mm. If it were to have a similar design to SCUBA-2 it would need to be 25mm thick and would have a central deflection of ~10mm. This would have unacceptable losses. An alternative would be to use a meniscus window. For a meniscus radius of 500mm and a thickness of 6mm, the central deflection

is 0.1mm and the factor of safety on failure of >10. Windows of this type and size have not been manufactured before and a technology development programme would be needed to make this possible.

10.3.2.4 Filters and Dichroics

The following filters are included in the optical design:

- 1 at 300K
- 3 at 60K
- 1 at 4K
- 1 in front of each detector at 1K

The filters at 300K, 60K and 4K all measure ~460mm CA – current largest filter for SCUBA-2 is 185mm CA. The filters are produced by the Astro-physics department of the University of Wales – Cardiff. They are currently set up to manufacture filters up to 300mm diameter and there would be considerable work and cost involved in setting up to manufacture these larger filters.

10.3.2.5 Focal plane units

The focal plane of the instrument has a diameter of 291mm. With a simple tessellation of the existing SCUBA-2 Focal Plane Units (see Figure 22) it is not possible to fit all the 16 sub-arrays that make up the focal plan into this space, as shown below. In order to achieve the required array spacing it is necessary to move each cluster in towards the centre by approximately 45mm. Further design work will be needed on the mK array readout wiring to prove this is possible, however at this stage there are no foreseeable issues prevent this. A likely outcome of this work would be that the sub-arrays will no longer be identical.

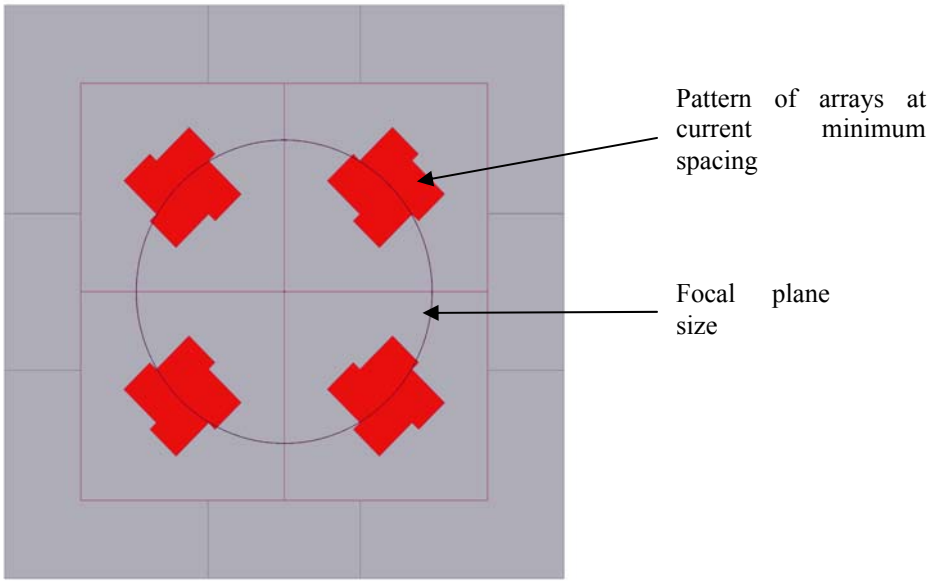

Figure 22: Simple tessellation of the existing SCUBA-2 Focal Plane Unit

The 3 focal planes are arrayed in the cryostat using dichroics to split off the wavelengths. See Figure 23.

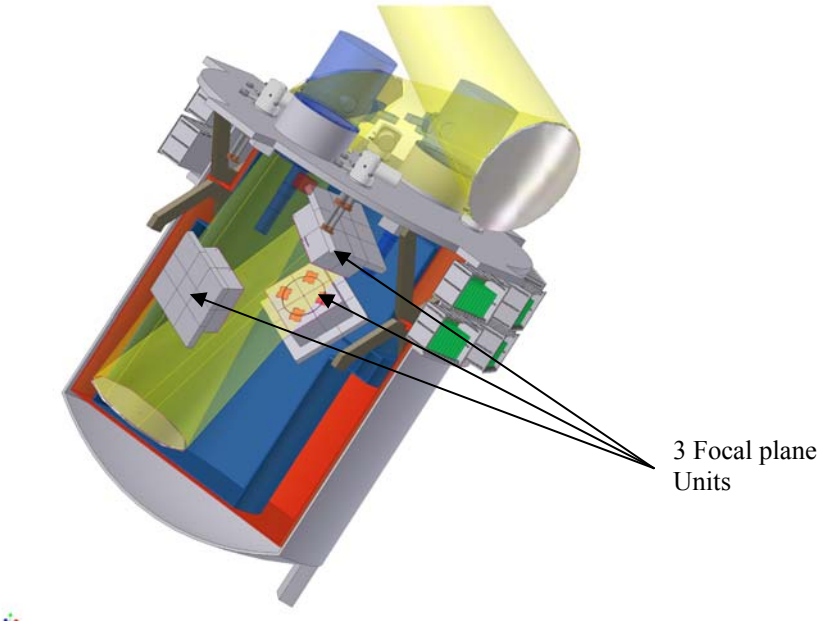

Figure 23 Cutaway of the cryostat showing the layout of the focal planes

Each sub-array requires a set of room temperature electronics mounted as close as possible to the cryostat. Figure 24 below shows a layout with 24 sets of electronics. The electronics design requires 48 sets of electronics, however this can be easily achieved by modifying the racks to accommodate the cards for 2 sub-arrays.

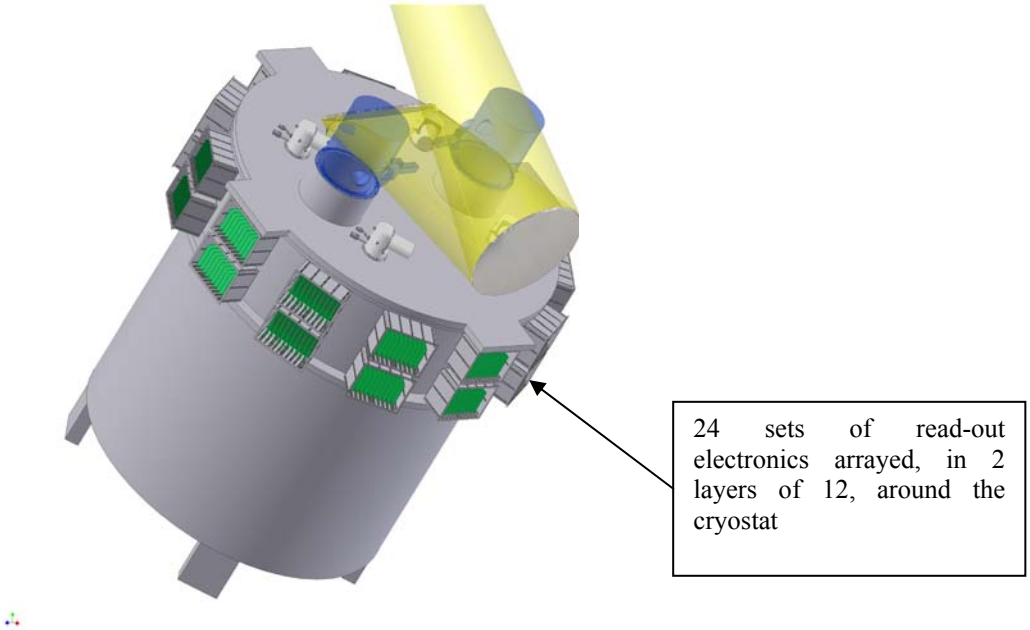

Figure 24 Layout of the warm electronics

10.3.2.6 Polarimetry wave plates

SCUBA-2 also has an add-on Polarimetry unit and it is desirable to have this facility on SCOWL. The SCUBA-2 wave plates are required to be ~300mm in diameter and a technology development programme is underway to achieve this. The only suitable position to mount a Polarimeter in the current design of SCOWL is on the top plate of the

vessel, between N1 and N2. This would dictate a wave plate size of ~850mm diameter. Currently there is no means of manufacturing these wave plates.

10.3.3 Space Envelope

During the period of the project, two different space envelopes have been provided for the SCOWL instrument. The OWL Telescope-Instruments Interface Control Document (AD02) and the Adaptor-rotator draft concept (RD03). These have been used together with the OWL Zemax optical model to define the space envelope. For modelling purposes, the space envelope in RD03 was used. With the current optical model developed it was not possible to fit the optics and cryostat within the space envelop as defined and we would require the envelop to be extended in toward the optical axis of the telescope by approximately 800mm.

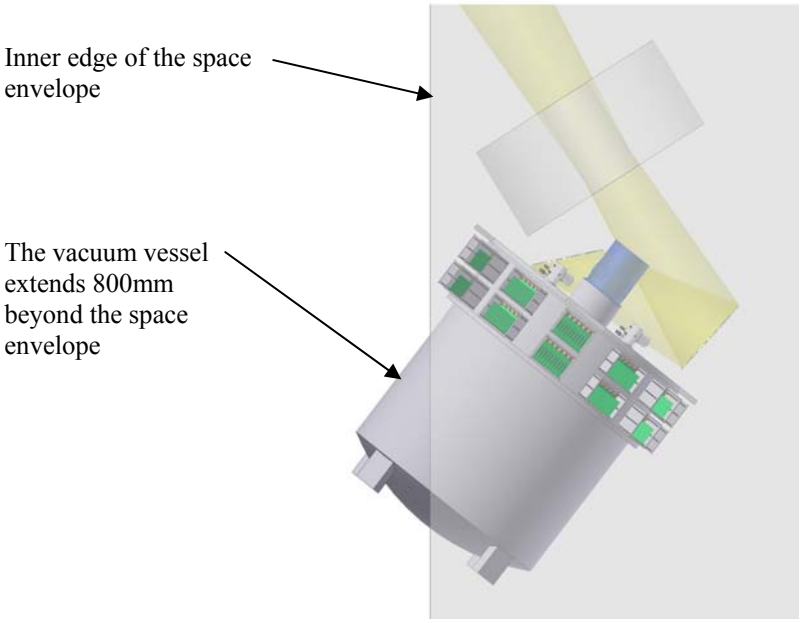

Figure 25: Space envelope

10.3.4 Cryogenics

10.3.4.1 Requirements

- The mirror N3 must be at a temperature of less than 15K to minimise thermal background at the arrays.
- A field stop at 1K is required to be mounted immediately in front of the arrays.
- The detector silicon temperatures are as follows:
  - 850µm – 130mK
  - 450µm – 190mK
  - 350µm – 250mK *(TBC)*

At 60K the heat loads on the cryostat are dominated by radiation through the window and walls of the vessel. The primary conduction load is through the trusses needed to support the large mass of the instrument. At 4K the heat loads are equally split between radiation and conduction, with the trusses again dominating the conduction load. At temperatures lower than 4K radiation can be ignored and only the conduction loads need to be considered. Support structures become much smaller and conduction through the array wiring becomes significant, especially in the case of the SCUBA-2 arrays where the detectors can only be multiplexed in one direction and the wire count is high. Fine wires are used to reduce the conducted load however this then leads to Joule heating within the cables when the arrays are operated, particularly at the lower temperatures. With the originally proposed Constantan wiring this Joule heating would have made it impossible to operate the array housing at the required 1K temperature. As a result we are now using Niobium Titanium (NbTi) wiring which becomes super conducting below around 9K. Provided the wires are

cooled to below this temperature through heat sinks on the 4K structure, Joule heating can then be ignored in the lower temperature stages.

SCUBA-2 uses Pulse Tube Refrigerators for the first and second stages of its cryogenic system and a Dilution Refrigerator for its third and fourth stages. Both of these technologies are gravitation vector dependant and are unsuitable for use on SCOWL as currently proposed.

10.3.4.2 1st and 2nd stages

- An LN2 pre-cool is assumed for the first and second stages of instrument. On SCUBA-2 this cools the instrument to 77K in approximately 48hours. Given suitably sized tanks and flow rates, a similar time should be achievable for SCOWL. A distributed flow system similar to that used on CRYRES could be adopted, however experience on SCUBA-2 has shown that using appropriate materials and careful design, the additional complexities of the distributed system can be avoided with no loss of performance. Ideally pre-cool will be performed off the telescope.
- PTRs lose performance when tilted. 30º is about the maximum without loss of performance for the PT410s used on SCUBA-2. Use of these fridges would require the instrument to be mounted on a Nasmyth platform. An alternative is to use a GM cooler, the performance of which is not orientation dependant. A suitable choice would be a Sumitomo SRDK-408D2, which has 44W at 40K on the 1st stage and 1.0W at 4.2K on the second stage when operated at 60Hz.
- At 60K the heat loads are dominated by radiation from the walls of the cryostat and through the window. Since the cryostat is twice the size of SCUBA-2, the heat loads should scale accordingly. SCUBA-2 was designed assuming radiation loads ($6.24 W/m^2$) in line with those measured on previous smaller instruments, however recent measurements on the cryostat have shown that for a larger blanket with a more optimised design, significant improvements can be made. As such, the expected radiation load will be $0.8 W/m^2$, which equates to 20W. In addition we would expect a further 20W of load through the window, and 20W of conducted load. A minimum of 2 coolers would be required to achieve the required performance.
- At 4K the load will be ~5W, of which approximately 50% is due to radiation. A minimum of 4 coolers would be required to achieve the required performance.

10.3.4.3 3rd and 4th stages

Detector ~ 0.1K and low temperature radiation shield ~1K
Scaling the SCUBA-2 design we can expect heat loads of ~6.5mW on the 1K stage and 150μW on the mK stage

- A closed cycle Dilution Refrigerator is the only real cost effective option for continuous cooling at these temperatures. Using the DRF design currently being built for SCUBA-2 we would require 6 units to cool all the detectors. Since the heat load is dominated by the array wiring, any reductions in this would reduce the number of coolers needed.
- Standard DRFs are dependant on a fixed gravity vector for operation, however DRFs for space applications are being developed which are gravitationally independent. Examples of these systems use mixing of ^{3}He and ^{4}He at a junction[7] or bubbles of ^{3}He in a ^{4}He bath[8] to provide the cooling power, however the maximum cooling power these can produce is typically only 1μW. The junction system in particular looks particularly promising as it should be possible to scale these coolers by machining many of these junctions into a block and circulating Helium through them in parallel to give higher cooling powers. This type of system also has the advantage that the point of cooling can be located right next to the object you need to cool rather than being some distance away, and requiring bulky thermal straps to transmit the cooling power. Whilst not reducing the required cooling power, it does mean that the cooler can run at significantly higher temperatures e.g. 80mK instead of 35mK, which is much easier to achieve. Currently these junction coolers are designed to run in an open cycle, however if the He mixture can be separated either within the cryostat or outside there is no reason why it cannot be run in a closed cycle.

[7] The performance of an open cycle dilution refrigerator. Adriana Sirbi, Alain Benoît, M.Caussignac and Serge Pujol. Proceedings of the 21st International Conference on Low TEMPERATURE Physics, 1996.
[8] Progress on a microgravity dilution refrigerator. Pat R. Roach, Ben P.M. Helvensteijn Cryogenics 39 1015-1019

- An alternative distributed mini-fridge DRF system[9] is currently being developed at Cardiff University. These fridges are not gravitationally dependant. This technology is still being developed but could be mature in time for a SCOWL instrument.
- Pre-cooling of these fridges is also an issue. The incoming Helium must be cooled in stages to about 4K otherwise it will provide too much heat load onto the system. Traditionally this is done using 77K liquid Helium and 4K liquid He baths followed by a pumped ^{4}He 1K pot. The large quantities of liquid cryogens required lead to high operating costs, particularly at a telescope site where liquid Helium is very expensive. For the SCUBA-2 fridge we have had a custom built system developed where by a PTR coupled to a Joule Thompson heat exchanger is used to provide the pre-cooling to ~2K. This has been shown to give very good cooling power. A GM cooler is much less suitable for this application due to the inherently large vibration levels. If these are not carefully isolated, they can lead to high levels of vibrational heating in the Mixing Chamber, significantly reducing the available cooling power.

Development of a dilution refrigerator which is gravitationally insensitive and has high cooling power is the key area of the mechanical design where significant development work is required if the SCOWL instrument is to be mounted on a Alt-az telescope. Alternatively, if the instrument can be mounted on a Nasmyth platform then existing technologies can be used.

10.3.5 Mass estimate

Table 13: Cryostat mass budget

Temp stage	Component	Mass(kg)
Vacuum Vessel	Vessel	1200
	Vessel lid	750
	Support frame	500
	Total	**2450**
Services	Services	200
	Compressors	800
	Coolers	200
	Total	**1200**
60K	Radiation shield	750
	Trusses	100
	Total	**850**
4K	Shield	500
	Mirror support	20
	Mirror	50
	Trusses	70
	Total	**640**
1K	Focal plane units	300
	Trusses	10
	Cooling straps	15
	Total	**345**
mK	Cooling straps	15
	Arrays	150
	Total	**165**
General Assembly	**Total**	**5650**

[9] http://www.astro.cf.ac.uk/groups/instrumentation/student_projects/refrigerator.html

The estimated mass is higher than the 4 tonne limit for an instrument mounted on the Instrument Rotator (RD03 Section 2.2), and is likely to increase significantly as the design develops. Unless the specified mass is increased it would not be possible to mount the instrument in this location. The proposed alternative heavy instrument attachment points at the corners of the instrument bay are a considerable distance from the closest parts of the instrument and a large stiff structure would be required to mount the instrument with appropriate levels of flexure. In order to minimise this additional mass it is proposed that a framework is provided at mid height within the bay, which instruments can be mounted off. A simple concept design is shown in Figure 26 below.

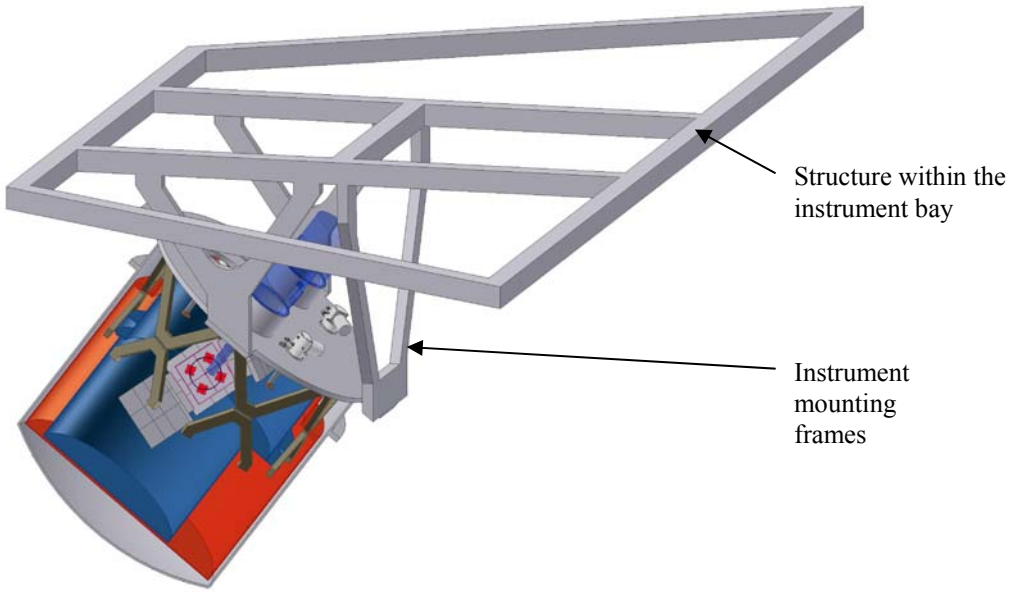

Figure 26 Instrument mounted on the proposed instrument bay internal framework

10.3.6 Flexure

The background source count is such that over a 2.5 arcmin FoV, there will be a few 1-3mJy sources at 850μm. The s:n on these in 1sec will be ~10σ, which may be bright enough to act as guide stars to remove slow flexure effects. See 9.2.1.3 for more details. However, the possibility that these sources may be extended needs to be investigated. There are not likely to be enough guide stars with *known* positions at submm to allow *absolute* pointing correction. Also the typical background source in the FoV is unlikely to be bright enough for rapid (<1second) control of pointing.
However, if it turns out after further investigation that submm flexure measurement using astronomical sources is impossible, there are other potential methods of flexure measurement and correction. The optical and submm beams are difficult to co-align and may not stay co-aligned. We propose to use a verified model of flexure to correct the pointing – either in real-time to correct the telescope pointing model, or offline in the data reduction. This requires regular submm pointing checks.

The flexure budget for SCOWL contains a reproducible term (which can be corrected, as described above) and a non-reproducible term (hysteresis, random changes) which could not be corrected without some other regular measurements.

10.3.6.1 Flexure budgets

The principle budget for flexure is that non-repeatable flexure shall remain at less than $1/10^{th}$ of a pixel. Given a pixel size of 1.135mm this equates to 0.1135mm. Exactly what this non-repeatable error is made up of will depend on what telescope instrumentation is provided and can only be speculated given the current state of the telescope design. The key factors, however, are likely to be as follows:

- Temperature stability within the instrument enclosure – due to the large scale of the instrument small changes of temperature could have large effects on the image position.

- Range of correction available in the telescope optics – this needs to be sufficient to be able to correct instrument flexure as well as telescope flexure.
- Precision of the pointing model
- Stiffness of the heavy instrument mounting fixtures – since the instrument is too large to fit on the instrument rotator as currently specified, there will be differential motion between the rotator and the instrument.
- Vibration levels within the instrument enclosure.

The estimates for SCUBA-2 are shown below. It can be expected that SCOWL would perform in a similar way:-

Table 14: Flexure estimates for SCOWL.

	X & Y decentres (mm)		X tilt (Degrees)		Y tilt (Degrees)	
	Budget	Estimated	Budget	Estimated	Budget	Estimated
Total	± 0.250		± 0.0699		± 0.0116854	
Correctable	± 0.125	± 0.032	± 0.040		± 0.040	
Dynamic	± 0.100	± 0.035	± 0.0095	± 0.0027	± 0.020	± 0.0027

Total – This is the total misalignment from a perfectly aligned system due to errors in static alignment combined with repeatable and non-repeatable motion.
Correctable – Flexure which can be corrected with a pointing model
Dynamic – Flexure which cannot be corrected with a pointing model

10.3.7 Handling

- Given the mass of the instrument as indicated below, it is expected that it will be moved from the technical rooms to the focal station using the side lift
- Compressors for the cool heads should be positioned remotely on the telescope at a position where there is no change of gravity vector.
- Experience with SCUBA-2 has shown that the instrument can comfortably be assembled and handled using two cranes mounted on a travelling beam (10 tonnes and 2 tonnes), and mounting points for suitable swivel lifting rings will need to be incorporated into the design.

10.3.8 Calibration

- SCUBA-2 uses a black body calibration source outside the window to flat field the arrays. Currently the largest available has a 300mm x 300mm square aperture which is too small. A system using multiple sources or a new single large source will be required.

- A 1K Cold Shutter is provided in front of the detectors to enable dark frames. The current design covers an aperture of approximately 100mm diameter, so a completely new design will be needed for SCOWL to cover the 291mm field.

10.3.9 Services

Cryogenics

- 4 Compressors for GM – 8KW plus 7 litres/min cooling water each.
- 6+ Gas handling systems for Dilution Refrigerators 2kW plus cooling water each.
- Thermometry for 60K, 4K 1K and mK stages
- LN2 supply for pre-cooling.
- Heater panel supply.

Vacuum systems

- Turbo pump control
- Backing pump
- Dry Nitrogen feed for the window

- Gauges and controllers

Mechanisms

- Motor drive cards for Cold Shutters and Calibration source
- Datum sensing for mechanisms

10.4 Electronics

10.4.1 Transition Edge Sensor (TES) Detectors

Recent advances in detector technology have demonstrated that large-format arrays of many thousands of pixels are now possible so that wide-field submillimetre imagers are more feasible. Indeed there are a few projects, currently underway, utilising the advances in this field. One of these instruments is SCUBA-2, a new generation camera under development for the JCMT. A substantial detector development programme, for SCUBA-2, is currently underway at the National Institute of Standards and Technology (NIST) and the Scottish Microelectronics Centre (SMC).

The current baseline detector, under consideration for SCOWL, is based on the SCUBA-2 design. The detectors are state-of-art transition edge sensors (TES) hybridised to a Superconducting Quantum Interference Device (SQUID) time-division multiplexer, shown in Figure 27.

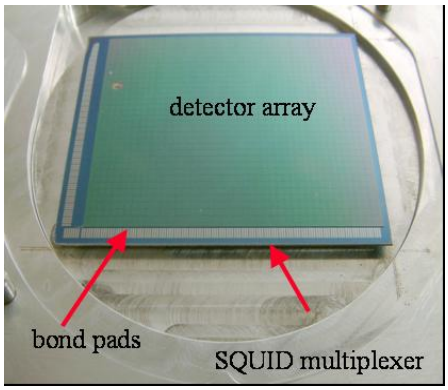

Figure 27: Hybridised detector/multiplexer

The TES is a superconducting thin film biased in the transition between the normal and the superconducting states. If biased in the transition region a small change in temperature will lead to a large change in resistance as shown in Figure 28. The detector is held at a constant voltage bias so that a change in resistance will cause a change in current which will be coupled into the SQUID readout.

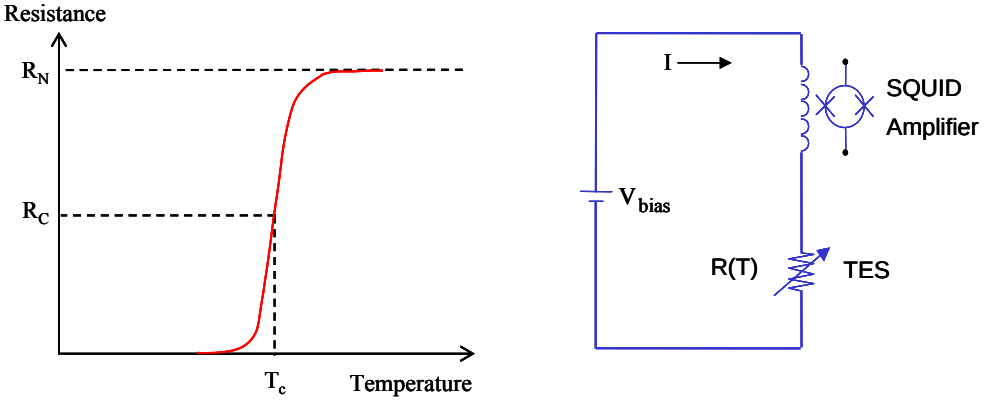

Figure 28: (a) R-T curve for TES device **(b) TES bias circuit**

The TES devices are low impedance and therefore less susceptible to microphonics and operate faster than conventional bolometers due to their high sensitivity and electro-thermal feedback mode of operation. The advantage of the SQUID multiplexer is that they consume less power than conventional FETs and operate at the same temperature as the detector. This last point is very important for arrays of detectors as it allows the readout of the pixels to be undertaken with a practical number of wires.

Without the advantage of multiplexing, each pixel would require 6 wires which would lead to >100,00 wires being routed from all of the detectors required for SCUBA-2, which would cause considerable problems in instrument building. Even with multiplexing a total of ~2500 wires are still needed to route signals to/from the detector arrays within the SCUBA-2 cryostat. For each detector subassembly there are a minimum of 320 connections required and SCUBA-2 has two focal plane units of four detectors each. A focal plane unit with the four detector subassemblies is illustrated in Figure 29.

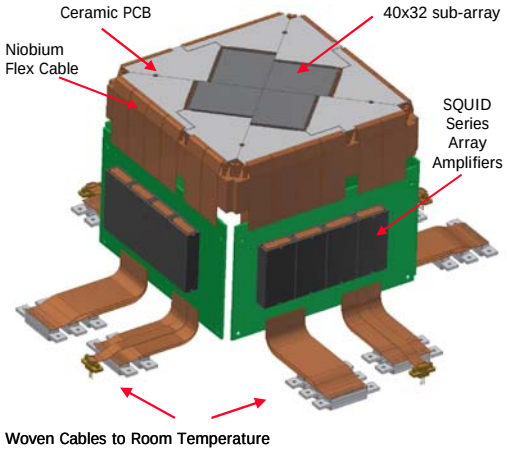

Figure 29: SCUBA-2 Focal plane unit

The specification of the current SCUBA-2 detector devices are as follows:

- Pixel size 1.135mm^2
- Physical size ~ 40mm x 50mm
- 1312 pixels per detector (40 rows x 32 columns + 1 'dark' row)
- 2 sides buttable – allows a mosaic of 4 detectors (5120 pixels)
- Operating wavelength: one mosaic at 450um and one mosaic at 850um
- NEP $_{(450um)} < 15x10^{-17}$ W/√Hz, NEP$_{(850um)} < 3.5 x10^{-17}$ W/√Hz
- SCUBA-2 FOV ~50-sq arcmins
- Operating temperature 100mK

To date, an 850um prototype detector has been fabricated and characterised and found to meet the required specification. A 450um prototype detector has also been fabricated. Science grade devices will have been delivered and tested to meet the instrument delivery date of mid 2006.

10.4.2 SCUBA-2 type detectors on SCOWL

In terms of the current SCUBA-2 array design there are four main issues to be overcome to realise even larger format arrays: (1) processing of silicon wafers (2) device density on the multiplexer wafer (3) power dissipation in focal plane (4) the large volume of readout wires.

Processing capabilities are limited to 3" wafers due to fabrication limitations within the project. This limits the number of rows of detectors to 40. Also, at present the size of wafers that can be successfully hybridised is about 50mm^2. Increasing the number of rows would also affect the multiplexing frequency which in turn affects the SQUID coil design. The detector is two edge butt-able, limiting the configuration to a mosaic of four.

The net effect of these factors is that to increase the size of this type of detector would involve further significant development work.

Wavelength range - Continuum detectors of this type are efficient at wavelengths between 200um to 1mm. The wavelength of operation is dependant on the geometry of the pixel, in particular the thickness will determine the operating wavelength. This in turn affects the absorption efficiency (which is equivalent to QE). The interdependencies of all the parameters and geometries is quite complex but detectors for operating at 350um, 450um and 850um are realisable.

The baseline design for SCOWL would be to forgo the costly and time consuming development work and use the existing SCUBA-2 design. Even with this approach dealing with the heat load, in the focal plane, from the increase in number of pixels and the increase in read-out wire count will be a challenge.

Figure 30 shows a schematic layout of four SCUBA-2 type detector subassemblies which would be required to cover the SCOWL field-of-view. This would give a total of 20480 pixels.

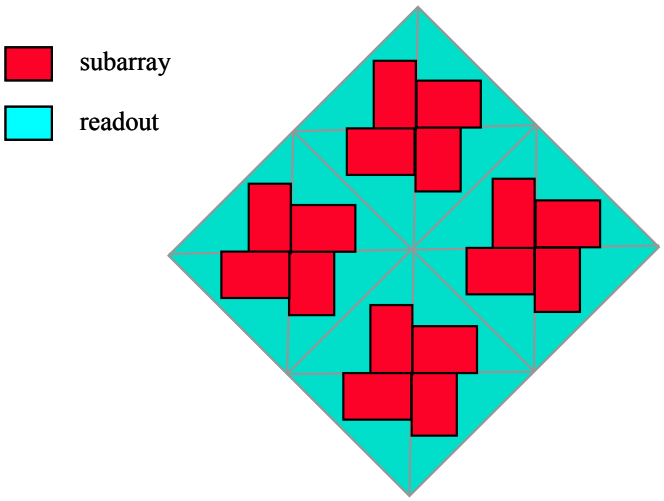

Figure 30: SCOWL Focal Plane schematic layout

With the present development programme, focal plane units consisting of 20k pixels are realisable. To significantly increase the number of pixels would require a substantial development programme and may be achieved in a timescale which will be of benefit to SCOWL

10.4.3 Readout Electronics

As shown in Figure 29 each detector is wire bonded to a ceramic PCB which is connected to a further PCB housing part of the readout electronics, the SQUID series arrays. This connection is made via niobium flexible circuits, which goes superconducting at temperatures below 9K. Cryogenic ribbon cables, constructed from niobium wires weaved with nomex fibres, route the signals to room temperature electronics. The detector output is DC-coupled to the readout electronics.

Mounted on the outside of the cryostat would be a VME rack containing all the circuitry to control and readout the detector. Fibre optic cables connect the warm readout electronics to a control and image capture PC running Realtime Linux.

Each VME rack contains a Clock Card, Address Card, 3x Bias Cards, 4 x Readout Cards, Power supply card and one VME rack will readout 1 detector therefore sixteen racks of electronics would be required for SCOWL for each waveband.

10.4.4 Kinetic Inductor Detectors (KIDs)

An alternative to the SCUBA-2 TES detectors for the detection of submillimetre radiation would be Kinetic Inductor Detectors (KIDs). They comprise a superconducting thin-film transmission line resonator. When a superconductor is operated well below its transition temperature (T << Tc) incoming photons are absorbed, breaking cooper pairs and creating a large number of quasi-particles. This increase in quasi-particles density changes the surface impedance, which is mainly inductive. This change in the surface impedance is measured by incorporating the superconductor into a LC resonant circuit. The change in surface impedance alters the resonance frequency and can be monitored by the RF readout system. By loosely coupling a large number of resonators operating at slightly different frequencies, to a single thin-film transmission line a large number of pixels (~1000) can be read out through a single HEMT amplifier and coax line. The number of frequencies that can be multiplexed depends on several factors (1) bandwidth of HEMT amplifier (2) typical Q of resonator (3) lithographic processes (4) exciting frequencies, to name a few. The advances made in wireless communication means that the RF readout and data acquisition could be implemented with mainly of-the-shelf components.

A number of international groups are working on developing KIDs. In the US groups at JPL and Caltech are working in this area as well as a group in the Cavendish Lab at University of Cambridge. Most of this work has concentrated on the X-ray region mainly because the high photon energies allow single-absorption events to be recorded rather than there being any reason that KIDs are more suited to working at this wavelength. Indeed KIDs can be configured to work at submillimetre, infrared, optical and X-ray wavelengths (RD07-10).

This technology is still in the early development phase but within the next 3 years it is likely that a 32 element system suitable for use in the submillimetre will be demonstrated, along with a suitable readout system that will scale to the larger format arrays.

The advantages of KIDs over TES detectors is that they are easier to manufacture and likely to be cheaper as the TES has the costly and complex hybridisation of the detector to the SQUID multiplexer. KIDs also have a future potential to be extended to large format arrays subject to ongoing development programmes.

Another advantage is that frequency multiplexing can be used to readout 10^3 - 10^4 detectors using a single HEMT amplifier thereby significantly reducing the heat load from the number of interconnections required as well as the practical problem of routing the connections through the cryostat.

The advantage of TESs over KIDs is that they have been shown to be effective in the submillimtre regime and are sufficiently far along in development but on the order of 3 years the KIDs development may be sufficiently mature to be seriously considered as an alternative to the TES detectors for SCOWL.

Summary of KIDs advantages:

- Easier to manufacture
- Wire count down, so simpler & more robust wiring design
- Fewer wires, so lower heat load
- Potential to fully populate the field of view, increasing the number of pixels by ~5
- Potentially cheaper to procure

10.5 Software

The software system block diagram assumes the telescope will adopt the usual architecture, whereby observation

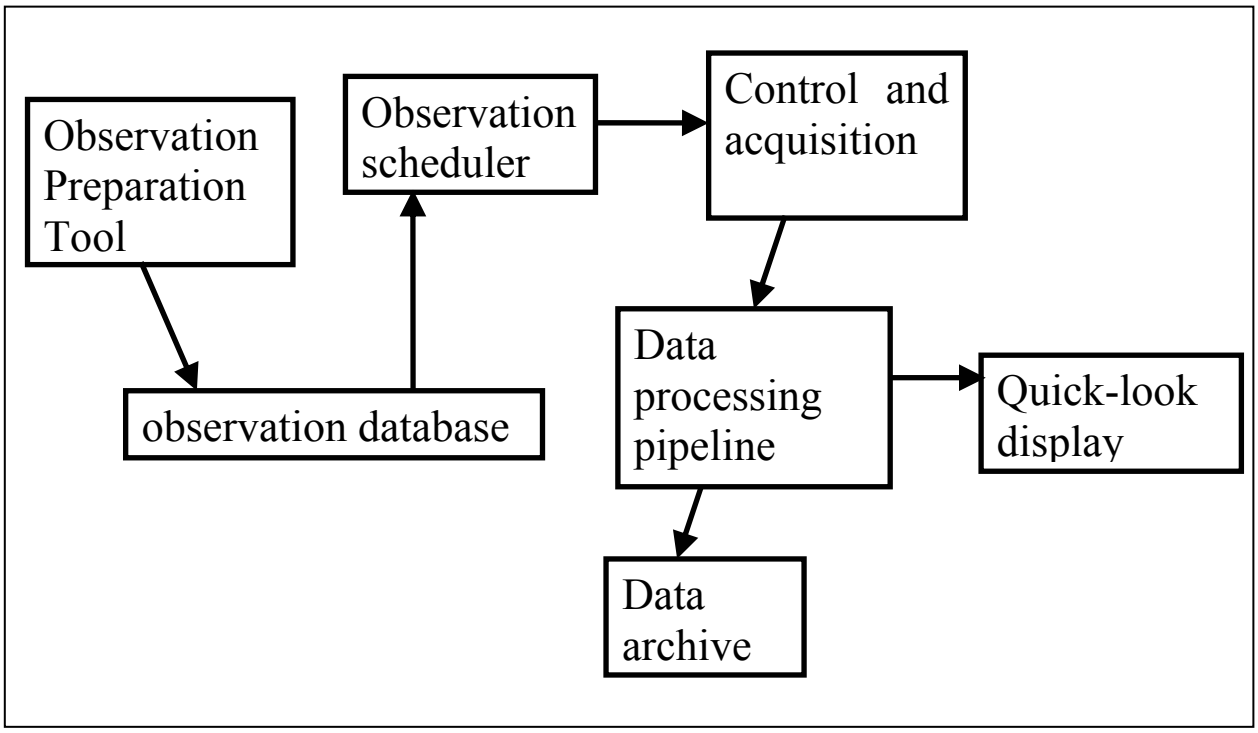

requests are prepared ahead of time and stored for subsequent recall at the telescope, and the data acquired are processed automatically by a data processing pipeline. As always, this carries the requirement that the data written by the control and acquisition subsystem contains all the information needed to drive the pipeline, including the identification of processing recipes if necessary.

11 Calibration

If TES devices are used, the exact calibration technique will depend on experience with SCUBA-2 on JCMT, from 2006 onwards. See section *10.3.8*. If other devices such as KIDS are adopted, the calibration technique is likely to be similar, although further modelling would be required.

11.1 Optimisation of Bolometer Loading

The bolometers are designed for optimal noise and response within a certain range of power input. The large variations in the emission from the Earth's atmosphere with time have to be compensated by a second source of power input to the bolometers which is adjusted in the opposite direction to variations in the atmospheric flux. This is achieved by having a heater resistor built into each bolometer and adjusting the electrical power supplied to the resistors so that the sum of power input from the heaters plus the illumination from the Earth's atmosphere is close to the optimal value.

11.2 Relative Calibration of Bolometers

The bolometers are nonlinear devices and their response curves are expected to differ slightly from bolometer to bolometer. In addition, drifts in electrical zero points can be expected.

A two-stage calibration technique is used involving the flat-field illuminator and the pixel heaters. The flat-field illuminator is used to record measurements from the bolometers at the working power loading with the heater input set to zero. The dark shutter is then closed, and measurements taken at a range of heater settings. This enables calculation of the relative resistances of the heaters to be determined. Thereafter the heaters can be used for direct determination of the zero points and response curves of the bolometers. It is advantageous to perform the calibration this way because the power input from the heaters is intrinsically lower noise than the photon noise present in an optical calibrator. Quick repeat calibrations can be carried out at frequent intervals during observing.

11.3 Extinction Correction

In the submm, atmospheric emission and extinction are both dominated by the opacity of water vapour. Therefore, there is expected to be a tight correlation between the flux recorded from the atmosphere and the extinction, and this is confirmed by detailed modelling. Provided an absolute calibration of the power received can be achieved, it becomes possible to calculate the atmospheric extinction directly from the sky background recorded in the science data frames. The calibration involves knowing the non-atmospheric flux present in science frames – this is normally grouped under the heading "telescope emission".

This technique is not yet standard and has to be proved using SCUBA-2. If it proves nonviable, then the system will require a water vapour radiometer to provide a measurement of the atmospheric extinction.

12 Management

The management aspects of this report are focussed on providing a first basic estimate of the cost for producing SCOWL. As such the estimate must be treated with great caution due to the very early stages of the concept. As SCOWL will be a brand new instrument, data on costs have been inferred by drawing comparisons with SCUBA 2 which is now in the AIV phase. Assumptions are provided to help establish the background to making the estimates.

12.1 Assumptions

The following assumptions have been made:

1. No allowance for inflation has been included; therefore all cost estimates are at 2005 prices.

2. A consortium based on the original SCUBA 2 team (or people with equivalent skill sets) is used to produce the detectors.

In global terms:

1. Overall design effort is expected to be of a similar order as for Scuba 2 with potential to reduce because of what has been learnt on SCUBA 2.

2. AIV in Europe is expected to be generally comparable to the effort for Scuba but will need to be scaled for the increase in effort required to integrate more detectors.

3. Activities at the Telescope site that could have a bearing on acceptance timescales of the Instrument have not been included (i.e. we assume for estimating purposes to avoid double accounting with the Telescope commissioning activities that all the infrastructure such as services and software is available).

12.2 Costs

The effort required to produce SCOWL has been provisionally estimated using the experience from the SCUBA 2 programme. It should be noted that there are three main sites involved with developing SCUBA 2 in the UK and one in Canada. In addition, essential input has been provided by other partners in the USA with regard to the detector technology. An exchange rate of €1.5 to the £ has been used.

- At present it is envisaged that effort would cost of the order of €9,000k.

- At present it is envisaged that hardware would cost approx €27,000k (of which €18,000k is for the detectors).

For SCOWL there are currently significant issues which have been identified for some of the hardware items which could necessitate an increase to these costs should dedicated R&D programmes funded by the project be required to solve manufacturing issues.

12.2.1 Contingency

An overall allowance for dealing with unknown risk must be included within the estimates. Current experience indicates that this should be of the order of an additional 20% for effort and 10% for hardware for a mature concept.

13 Conclusion

SCOWL is a concept for a large-format sub-millimetre camera to be used on the OWL Telescope. Such an imager would be unique, more sensitive than any other facility, and be able to map large areas of sky a million times faster than ALMA. The results would impact a wide range of research. It could answer some of the most fundamental questions about the *origins* of dust, planets, stars and galaxies, and would significantly increase the scientific return from the OWL telescope.

The basic design goal of SCOWL is to fully pave the 2.5 arcmin science field of view with Nyquist-sampled pixels, giving sky-limited sensitivity at all three primary submillimetre wavebands (350, 450 and 850μm). The angular resolution will be 1-2 arcsec - sufficiently high that confusion limits will be three orders of magnitude below current telescopes. The huge OWL collecting area (effectively larger than ALMA) and high sensitivity means it will be possible to image objects at the 10μJy level at 850μm, more than two orders of magnitude better than existing instruments. At the shorter wavelengths, assuming a precipitable water vapour (pwv) content above the OWL site of 0.5-1 mm, a point-source sensitivity of 100-200μJy (10σ/1hr) at 450μm will be reached. This will degrade to ~1mJy (10σ/1hr) if the pwv is 2mm, and indicates that a high dry site such as Mauna Kea or Chajnantor would maximise the potential of SCOWL. As well as three-band imaging, SCOWL will also have a polarimetry capability.

Although SCOWL and ALMA will both operate in the submillimetre, their capabilities are clearly different. ALMA will be the facility of choice for the high resolution studies. But SCOWL will be the only instrument capable of deep widefield mapping. For example, at 850μm SCOWL will be able to map 1 square degree down to 1σ=40μJy within 10 observing nights, while ALMA even if it were possible would need 10Myr! Observing large sky areas in the submillimetre to high depth become feasible *only* with SCOWL. As such, SCOWL would also act as a pathfinder, searching for new objects for high-resolution followup with ALMA.

The baseline design of SCOWL uses the same basic system as SCUBA-2, currently the cutting edge of submillimetre continuum cameras. This is the lowest risk approach, and uses 48 of the existing TES detector arrays with a total of ~20,000 pixels at each wavelength to partially pave the field of view. However, to achieve the design goal of full coverage of the field of view, as well as relieve difficulties with cooling power and potentially reduce cost, an alternative detector technology - Kinetic Induction Detectors - may prove to be more capable. Although this will require a technology development program, the long-term advantages are likely to be considerable.

Annex 1: Technology Development Areas

The following table lists the issues that have been identified so far during the study on SCOWL. Cross-references to sections in the text where the issues are discussed are provided.

#	Issue	Comment	Section Cross-Reference
1	Size of input window that can be manufactured	Needs Technology Development Programme	10.2.2.3
2	Size of filters and dichroics that can be manufactured	Current size of SCUBA 2 filters are approx 200mm; 300mm is possible but 455mm is needed for SCOWL Needs Technology Development Programme	10.2.2.4
3	Polarimetry wave plates	Need waveplate of ~850mm diameter, no means of manufacturing this just now Needs Technology Development Programme	10.2.2.5
4	Waveplate rotation	Fast (2Hz) rotation of a large waveplate would be needed.	10.2.3.5
5	Detector Coolers	Dilution Refrigerator used for SCUBA 2 is gravity dependent; alternate cooling may be possible - is being investigated, if this does not work then a Technology Development Programme will be required	10.2.3.3
6	KIDS or alternative detectors	Development of alternative detectors has the potential to reduce cost and complexity of cooling. An improvement in performance is also likely due to increased packing density .	10.3.4

Annex 2: TELESCOPE REQUIREMENTS GENERATED BY SCOWL

The following system level requirements have been identified as being necessary to allow SCOWL to gather the science based on the presented concept. This should help contribute to the system level trade-offs debate.

#	SCOWL System Need	Resulting System Requirement	Comment
1	SCOWL has the potential to be used during daylight	Means of telescope tracking during daylight required	
2	Potential hitchhiker mode	Sub-mm/optical-ir dichroic	
3	Scanning velocity and acceleration	Velocity: 50arcsec/sec (max) 15arcsec/sec (typical) Acceleration: 100arcsec/sec/sec	For scan mapping. The maximum scan rate gives critical sampling by a single bolometer, but oversampling and a slower scan rate is preferred. The key thing is that the telescope instantaneous position must be well-determined.
4	Site quality (pwv)	≤1mm PWV	For 450 & 350μm operation
		≤2mm PWV	For 850μm operation
5	Submm seeing	<0.5 arcsec needs method of sub-mm "tip-tilt" correction	See section 9.2
6	Instrument Rotator	Not required for SCOWL	
7	Space Envelope	The SCOWL mechanical design envelope sits outside the current envelope by 800mm	ICD differs from Zemax file - updates will provide more stable start point.
8	Flexure		Flexure may be a risk area - solution may be to mount on a Nasmyth platform. See section 10.3.6
9	Stable Gravity vector	If cooling is shown to be an insurmountable problem, may require mounting Nasmyth platform.	3rd and 4th stage cooling of the cryostat at the detectors *may* require stable gravity vector.